
# RADIO FREQUENCY EMITTER GEOLOCATION USING CUBESATS

THESIS

Andrew J. Small, Captain, USAF

AFIT-ENG-14-M-68

**DEPARTMENT OF THE AIR FORCE**
**AIR UNIVERSITY**

***AIR FORCE INSTITUTE OF TECHNOLOGY***

**Wright-Patterson Air Force Base, Ohio**

AFIT-ENG-14-M-68

# RADIO FREQUENCY EMITTER GEOLOCATION USING CUBESATS

THESIS

Presented to the Faculty

Department of Electrical and Computer Engineering

Graduate School of Engineering and Management

Air Force Institute of Technology

Air University

Air Education and Training Command

in Partial Fulfillment of the Requirements for the

Degree of Master of Science in Electrical Engineering

Andrew J. Small, B.S.E.E.

Captain, USAF

March 2014

AFIT-ENG-14-M-68

# RADIO FREQUENCY EMITTER GEOLOCATION USING CUBESATS

Andrew J. Small, B.S.E.E.
Captain, USAF

Approved:

| | |
|---|---|
| //signed// | 13 March 2014 |
| Maj Marshall Haker, PhD (Chairman) | Date |
| //signed// | 7 March 2014 |
| Jonathan Black, PhD (Member) | Date |
| //signed// | 13 March 2014 |
| Richard Martin, PhD (Member) | Date |

AFIT-ENG-14-M-68


## Abstract

The ability to locate an RF transmitter is a topic of growing interest for civilian and military users alike. Geolocation can provide critical information for the intelligence community, search and rescue operators, and the warfighter. The technology required for geolocation has steadily improved over the past several decades, allowing better performance at longer baseline distances between transmitter and receiver. The expansion of geolocation missions from aircraft to spacecraft has necessitated research into how emerging geolocation methods perform as baseline distances are increased beyond what was previously considered. The Cubesat architecture is a relatively new satellite form which could enable small-scale, low-cost solutions to USAF geolocation needs.

This research proposes to use Cubesats as a vehicle to perform geolocation missions in the space domain. The Cubesat form factor considered is a 6-unit architecture that allows for 6000 $cm^3$ of space for hardware. There are a number of methods which have been developed for geolocation applications. This research compares four methods with various sensor configurations and signal properties. The four methods' performance are assessed by simulating and modeling the environment, signals, and geolocation algorithms using Matlab.

The simulations created and run in this research show that the angle of arrival method outperforms the instantaneous received frequency method, especially at higher SNR values. These two methods are possible for single and dual satellite architectures. When three or more satellites are available, the direct position determination method outperforms the three other considered methods.

## Table of Contents

Page

Page

## List of Figures

Figure Page

## List of Abbreviations

RADIO FREQUENCY EMITTER
GEOLOCATION USING CUBESATS

# I. Introduction

The problem of RF transmitter geolocation has been a topic of interest for military and commercial applications since shortly after World War II. The technology began with purely land-based apparatus, designed to find the direction of arrival by comparing the power of received signals among apertures in antenna arrays. The technology has since matured and been applied in more diverse areas, especially in the last several decades as communication technology has grown more rapidly. The geolocation platforms have also expanded from land-based to sea- and air-based, and are beginning to be applied in space-based applications.

Applications for geolocation techniques are wide ranging, and include both civil and military uses. The growth of civilian cellular networks makes geolocation ideal for services such as targeted advertising [1], E911 [2], roadside assistance, and other emergency services. Military applications include the geolocation of communication systems, GPS jammers, radars, and search and rescue efforts.

The applications which require geolocation lend themselves well to the space environment for several reasons. A space-borne geolocation system has a very large field of view, and can receive signals from a large region of the Earth. There are no restrictions on over-flying an area from space, as there would be from the air. Satellites do not require refueling, and can stay in orbit for years performing the mission with minimal human intervention. Surveillance of remote areas may also be easier for satellites, as weather does not become an issue in space.

## 1.1 Problem Statement

The goal of this thesis is determine if emerging methods of geolocation (direct position determination, instantaneous received frequency, time difference of arrival, angle of arrival) can be used in a nanosatellite based system. The performance these geolocation methods is to be compared by modeling and simulating the space environment. A set of scenarios is to be constructed to provide different circumstances in which the modeled satellites would perform the geolocation mission.

## 1.2 Current Research

A set of satellites which receive a signal from the ground will have several parameters which can be measured to estimate the location of the transmitter. The time at which the signal is received by the satellite can be used in a time of arrival (TOA) algorithm, and the time differential between signal reception can be used to determine the time difference of arrival (TDOA). The phase difference in an array of antennas can be used to determine the angle of arrival (AOA). The frequency difference of arrival (FDOA) can be measured to estimate the coordinates of the emitter. All of these parameters can be measured and then used to estimate the position of the emitter. This is a two-step approach, which is the classical method for geolocating a transmitter.

Recently, single-step methods have been suggested to improve performance of the geolocating system. Single-step methods gather the sampled signals at a single node or a separate processor to estimate the position of the transmitter without extracting the parameters separately. The Direct Position Determination (DPD) method is a promising new area of research that provides improved performance in the presence of noise.

Research into methods which are able to determine a transmitter's position with a single moving sensor has gained interest recently as well. The Instantaneous Received Frequency (IRF) method is a new technique which uses the Doppler of a moving sensor to

estimate the position of the transmitter. The method requires only a single satellite with a single antenna, which is ideal for the small space available in a Cubesat.

## 1.3 Scope and Application

This research investigates several possible methods for implementing a geolocation system in a set of nanosatellites. Several geolocation methods are discussed, and simulations of their use in the space environment are presented. This research seeks to provide baseline simulations that compare the performance of several geolocation methods. A set of variables will be included to assess the usefulness of the algorithms in differing conditions. This research is performed to inform a nanosatellite designer on the effectiveness of these algorithms if a geolocation mission is desired.

## 1.4 Assumptions

There are some limitations that are present in this research. The transmitter is assumed to be stationary, and its location is generally known, within a bounding box that is definable in the simulation. For example, the location may be assumed to be in or near a city, so the bounding box could be modeled as 1000 $km^2$. The signal structure is unknown, but the transmitted frequency is known. It is assumed that there are no other transmitters within the target box which are transmitting on the same frequency, or alternately that the geolocation system is able to distinguish the signal of interest from others received. The signal is assumed to reach the satellite with enough power to be received and processed effectively.

## 1.5 Methodology

A number of current geolocation methods are modeled to simulate the reception and processing of signals on-board a satellite. The simulated signals are attenuated, delayed, and frequency-shifted to represent a real-world signal passing through the atmosphere accurately. Once the signals are simulated as being received by the sensors, they are

processed using one or more of several possible geolocation algorithms. These methods are all presented in current literature on this subject, though use of these algorithms in a satellite or at the standoff range of a satellite may be a new application. The methods are simulated in Matlab to provide an estimate of the transmitter's position, which is compared to the true position to find the error and variance of the method over multiple runs. In addition to the average error of the methods, other factors such as performance at different signal to noise ratios (SNR's), satellite constellation configurations, and performance factors are explored.

## 1.6 Research Benefits

There are currently no nanosatellites on orbit which are performing a geolocation mission. This research intends to take a step towards enabling such a mission to exist. The algorithms presented in subsequent chapters of this thesis can be put to use in a Cubesat, and can be further modified to suit the needs of the user. United States Air Force (USAF) and Air Force Institute of Technology (AFIT) researchers can continue to improve on the work presented herein to make it more robust. The capability to passively geolocate a terrestrial transmitter from space will aid in mapping out Command, Control, and Communications (C3) nodes and creating Operational Plans (OPLANs). Geolocation of hostile jamming sites will aid the operational community by promoting rapid reconfiguration of navigation aids. Search and rescue operations may be enhanced, especially in remote areas.

## 1.7 Thesis Organization

Chapter I introduces the topic of geolocation, and provides an overview of the research conducted. Chapter II provides background information and addresses the current state of geolocation technology. Chapter III introduces the methodology used to simulate the satellite working to geolocate the signal source in the expected environment.

Chapter IV discusses the results of simulations. Chapter V presents conclusions from the research and details possible avenues of future research.

# II. Background

GEOLOCATION of radio frequency (RF) signals can be defined as "the problem of precise localization (or geolocation) of spatially separated sources emitting electromagnetic energy in the form of radio signals within a certain frequency bandwidth by observing the received signals at spatially separated sensors" [3]. Geolocation of signals is an important capability for military and civilian users alike. Increasing the accuracy of location estimates of a target RF emission will lead to more accurate targeting, better intelligence for the warfighter, and enhanced search and rescue effectiveness. Civilian programs like E911 [4] have already made use of geolocation methods to make tracking cellphones a reality. The E911 program has put in place infrastructure which can calculate a geolocation estimate every time a cell phone connects to a 911 operator. The program has opened the doors to research into improving solutions to geolocation problems. This research aims to add a robust solution making use of nanosatellites ("Cubesats") to the rapidly growing research area.

This chapter details the state of the art in geolocation techniques. Literature in the field of geolocation describes the various methods to locate the origin of a signal both passively and actively. This research will focus on the passive geolocation problem, with emphasis on the implementation of these methods in a geolocation system involving a constellation of Cubesats. Sections 2.1 and 2.2 give an introduction to the algorithms used for geolocation. Section 2.3 details the mathematical foundation of geolocation solutions. Section 2.4 discusses the primary sources of error in a geolocation system. Section 2.5 provides some performance metrics which are used to evaluate the algorithms. Sections 2.6 to 2.7 give the reader a primer on Cubesat systems and their capabilities.

## 2.1 Classical Methods for Locating Emitters

There are a number of methods for estimating the position of a transmitter given the reception of its signal across a set of sensors. There are four methods referred to in this thesis as the 'classical methods' - angle of arrival, time of arrival, time difference of arrival, and the frequency difference of arrival method [4]. These methods take a two step approach to formulate a position estimate. Each method first calculates some parameter based on the received signal features, then computes a best fit estimate of the transmitter's position based on each sensor's reported parameters. Classical methods are discussed further in this section, and Section 2.2 gives more information on alternative methods. Subsection 2.1.1 presents the AOA method, 2.1.2 discusses the TOA method, 2.1.3 introduces the TDOA method, and 2.1.4 presents the FDOA method.

### *2.1.1 Angle of Arrival.*

The AOA method solves the geolocation problem by determining a Line of Bearing (LOB) from each sensor to the target [5]. The LOB can be created by measuring the phase differences between a set of received signals from a phased array antenna. A steering vector defines the sensor's best guess at the precise angle at which the signal arrived. The method requires at least two LOBs for a position estimate to be made. Alternately, a single mobile receiver can be used. A mobile receiver has the ability to simulate multiple stationary receivers by taking measurements in different positions over time, provided the position and velocity of the sensor at each time epoch are known. The LOBs intersect at the estimated point of signal origin on a 2D plane or 3D surface, as shown in Figure 2.1. Additionally, the sensors for a satellite-based system are expected to be several hundred kilometers away from the transmitter at their closest point. Longer distances between sensor and transmitter will reduce the error margin that can be allowed in the angle measurement. The AOA method requires a minimum of one satellite and does not require time synchronization between the receiver and the transmitter for an accurate

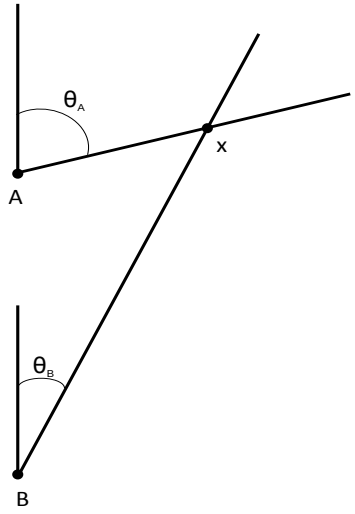


Figure 2.1: The Angle of Arrival method requires at least two lines of bearing to calculate the point of intersection [4].

measurement. Both of these characteristics make it an appealing method for an inexpensive passive geolocation system. One disadvantage of the AOA method is that position estimates are significantly degraded when the line of sight (LOS) signals are interfered with by the reception of Non-Line of Sight (NLOS) signals. In the context of this research, NLOS is not believed to be a vital concern because the detection will generally be done by space-based receivers with direct line of sight to the transmitter. The AOA method is studied primarily for its ability to geolocate with a single satellite.

### *2.1.2 Time of Arrival.*

Another method to geolocate an RF emitter is TOA, which measures the time a signal arrives at a receiver [4]. Given the signal travels at the speed of light, $c$, the distance traveled can be calculated from the propagation time. A circle of infinitely many possible emission locations can be drawn around the receiving sensor based on the calculated distance that the signal has traveled. Adding receivers will reduce the ambiguities of the

method by creating intersections along the circle. Thus, a group of three receivers can pinpoint an emitter in 2-D as shown in Figure 2.2.

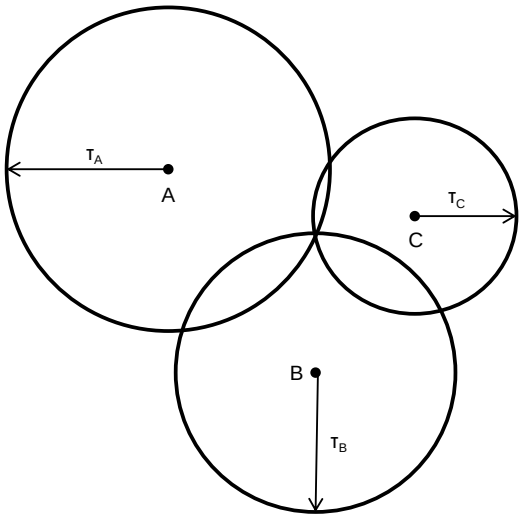


Figure 2.2: The Time of Arrival method uses a signal's propagation time to measure the distance the signal travelled. The position estimate is the point in space where the three location estimate rings meet [4].

The TOA method requires more receivers than the AOA method - three for a two-dimensional position estimate, and four receivers for a three-dimensional estimate. Additionally, the TOA method requires a detailed knowledge of the signal structure to estimate the signal propagation time. TOA depends on precision timing between the signal source and the receiver. This research focuses on the geolocation of non-cooperative receivers, which requires the assumption that accurate timing between transmitter and sensor is unavailable. For this reason the TOA method will not be used in this research.

### *2.1.3 Time Difference of Arrival.*

The TDOA method is perhaps the most widely used method for geolocation [6], [7]. This method uses the elapsed time between signal receptions at two or more receivers to estimate the emitter's position. Rather than drawing location estimate rings around a receiver (as in the TOA method), the TDOA method creates hyperbolic curves to represent the possible locations. The equation for the hyperboloid $R_{i,j}$ is as follows [8]:

$$R_{i,j} = \sqrt{(x_i - x_t)^2 + (y_i - y_t)^2 + (z_i - z_t)^2} - \sqrt{(x_j - x_t)^2 + (y_j - y_t)^2 + (z_j - z_t)^2} \quad (2.1)$$

where the points $(x_i, y_i, z_i)$ and $(x_j, y_j, z_j)$ are the coordinates of the receivers, $i$ and $j$, and $(x_t, y_t, z_t)$ are the coordinates of the transmitter. Figure 2.3 illustrates an example of how these hyperboloids can be used for geolocation. Like the TOA method, TDOA requires

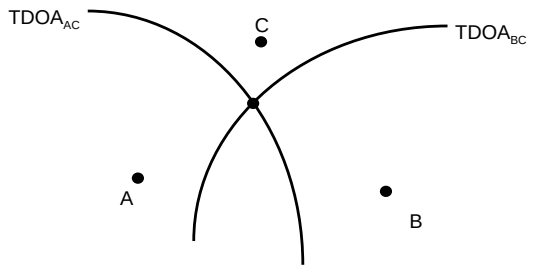


Figure 2.3: The Time Difference of Arrival method determines location by measuring the difference in reception time between two sensors, creating hyperbolas of possible location estimates [4].

three sensors for a two-dimensional estimate and four sensors for a three-dimensional estimate. The intersection of two or more hyperboloids gives the estimate of the signal source.

TDOA has many benefits for use in passive, space-based geolocation systems in comparison with the other methods discussed. TDOA does not require a common clock between the transmitter and receiver, making transmitter timing inconsequential. The only relevant time measurements are those between receivers, so it is critical that receiver timing remains synchronized [9]. Another benefit of TDOA is the simplification of the LOS/NLOS relationship. So long as there is one line of sight measurement, all others will be neglected if the leading edge of the waveform is used to determine the TOA. However, problems arise when there is no LOS. Position estimation is severely degraded when no direct path exists because the receiver will treat the first signal it receives as the LOS signal. Without LOS, the first signal will originate from a multipath reflection. With a space-based system, NLOS scenarios are assumed to be minimized, but can still occur in urban canyons. Various NLOS mitigation techniques and algorithms are presented in [4], and NLOS mitigation techniques are not a consideration in this research. TDOA is studied for its well developed algorithms and common use in systems with multiple sensors at differing baseline distances.

#### *2.1.4 Frequency Difference of Arrival.*

The FDOA method, also referred to as Differential Doppler (DD), measures the difference in frequency of a received signal between two or more receivers, much like the TDOA method does with time [4]. FDOA methods therefore require movement of either the signal source or the receivers. The shift in frequency is used to obtain a distance estimate by using the relation between the signal's speed, $c$, and the length of the waveform. FDOA estimation can be visualized by drawing wavelength curves around the receivers and finding points of intersection, as shown in Figure 2.4.

Noise will degrade the accuracy of the estimate. The velocity of the emitter and/or receivers can also cause poor performance if the movement is not at a sufficient speed to generate a measurable Doppler shift. Velocity issues will not be a significant factor in the

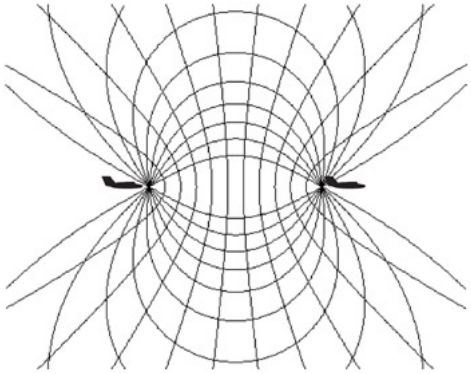

Figure 2.4: The Frequency Difference of Arrival method requires a moving transmitter or receiver to make use of the Doppler shift in the received signal [10].

research in this thesis, as a satellite in LEO will travel at approximately 7,500 km/s, ensuring a measurable difference in estimated frequency over time. In many systems, FDOA techniques are included as a supplement to methods such as TDOA and AOA, rather than as a stand-alone solution [7].

## 2.2 Alternative Methods

In addition to the classical methods discussed in the previous sections, new methods have been developed to improve on some of the inefficiencies and pitfalls of the classical methods. One such method is the Direct Position Determination (DPD) method, which uses a single step cost function approach to process the signals and determine an estimate. DPD and other alternative methods are often founded on classical methods, but have performance enhancements that distinguish them. Other alternative methods abandon the classical approach altogether in favor of a new paradigm.

A common approach is to use a hybridization of the classical methods to improve accuracy and robustness. By combining TDOA and AOA methods, for example, a system can generate estimates based on timing and lines of bearing, then use a best fit model to combine the two sets of measurements. Such a system will be more robust by taking

advantage of the benefits of both AOA and TDOA, while mitigating the negative aspects of each. In addition to hybrid systems, other methods have been developed to minimize the specific disadvantages of some systems in order to improve the results [11] - [14]. The Direct Position Determination method is a new approach that is rising in popularity [15] - [18] due to its single step solution and improved performance at low SNR, relative to the classical approaches.

### *2.2.1 Direct Position Determination.*

The DPD method improves upon the classical methods through centralized processing of the received signal. Weiss posits that there is error inherent in classical algorithms because received signals are not related to one another in processing [18]. Signals are processed separately, then compared to find their intersection. In order to eliminate this error, the signals must be referenced to one sensor. The DPD method improves position accuracy, most significantly at low SNR, but at the cost of increased computational complexity at a single node. Computational complexity presents problems in implementation due to the increased cost for required processing power, as well as the reliance on a single sensor or ground node for the majority of the work. Pourhomayoun and Fowler have modified the process to distribute the calculations among all sensors in the solution [16]. By using a Gershgorin Disc, eigenvalues can be approximated to reduce the calculations required. Additionally, they propose an algorithm that approximates the DPD while using a distributed processing model to accomplish the calculations. Their results show that the method is nearly equivalent to the original DPD method, and still more accurate than classical solutions.

The DPD method has been well developed for cases when the distance between the transmitter and receivers is less than 10 km. Generally, the solution space is in two dimensions. The application of the DPD method to a space system which takes measurements as far away as 1000 km, and with a solution in three dimensions has not

been identified in literature up to this point. This thesis is believed to present the first performance consideration of this expanded scenario.

### *2.2.2 Instantaneous Received Frequency.*

The instantaneous received frequency (IRF) method is related to the FDOA method described in Section 2.1.4, but instead of computing the difference in Doppler frequencies of a signal received by different sensors, the instantaneous received frequency is calculated. A moving sensor with a stationary transmitter will have a velocity which changes relative to the transmitter's position. The relative velocity of the satellite will change the frequency of the received signal. As the satellite moves toward the emitter, the received frequency will be higher than the transmitted frequency. This phenomenon reverses as the satellite moves away from the transmitter, and the received frequency will be lower. Geolocation can be performed using this information by matching the measured instantaneous frequency to Doppler values calculated from a grid of possible emitter locations. Nelson and McMahon [19] present a method which makes use of these principles. The method is attractive for a nanosatellite mission because it can work with a single receiver equipped with a single payload antenna. This research presents the first simulated performance of the IRF method in a scenario with space-borne sensor platforms.

## 2.3 Geolocation Problem Formation and Solution

Whether using a classical two-step approach or a single step approach, the parameters needed to solve for the transmitter's position remain embedded in the signal received at the sensors. Torrieri [5] details an iterative solution, and Ho and Chan [8] provide a closed form solution for the classical methods. Weiss [18] developed the single step method which will be used for the portion of this research dealing with DPD. Nelson and McMahon [19] provide the mathematical background for the IRF method which is utilized in this research as well. The following sections will delve into the mathematical basis for each of these methods in more detail.

### *2.3.1 Classical Step 1: Parameter Calculation.*

The classical solutions calculate a parameter such as the range or the angle between the receiver and the transmitter. Torrieri divides the estimation methods into two categories: hyperbolic location systems and direction-finding location systems [5]. Hyperbolic systems use methods such as TDOA and FDOA to locate a transmitter by processing signal arrival time measurements at three or more locations. Direction finding systems use methods that create bearing lines either at multiple stations or using the same station at different locations. A mobile receiver with a known trajectory is presumed for single receiver calculations.

#### *2.3.1.1 Hyperbolic Systems.*

Hyperbolic location systems compare the timing of signals received at spatially separated sensors to create a hyperbola of possible emission locations with focii at the sensors [5]. Adding stations determines the position estimate by finding where hyperbolas cross. An important aspect of this method is that the need for finding the transmit time, $t_0$, is eliminated because the only timing that is needed is the reception time difference between the two sensors, $\tau$. One exception is if the transmitter is producing pulses rather than a continuous waveform - in that case, care must be taken to ensure that the time between measurements is smaller than the time between pulses. Equations to describe the signals that two sensors receive, $x_1(t)$ and $x_2(t)$, are as follows [5]:

$$x_1(t) = s(t) + w_1(t) \tag{2.2}$$

$$x_2(t) = \alpha s(t - \tau) + w_2(t) \tag{2.3}$$

A signal $s(t)$ arrives with a time shift $\tau$ at one sensor, an attenuation factor $\alpha$, and some noise $w$ which will be modeled as white Gaussian noise. The value of $\tau$ can be measured by comparing the reception time of one sensor with another. Therefore (2.2) and (2.3) can be replaced by establishing the time difference between sensors $i$ and $i + 1$ as $t_i - t_{i-1}$. The

resulting equation is the following [5]:

$$t_i - t_{i+1} = \frac{\Delta D}{c} + w \tag{2.4}$$

where $\Delta D = D_i - D_{i+1}$, $D_i$ is the distance from receiver $i$ to the transmitter, and $w$ is noise. In (2.4) the time values can be measured. The noise value can be modeled stochastically, and is assumed to be white Gaussian noise. The only unknown in (2.4) is $\Delta D$. By measuring the reception time at each receiver, solving for $\Delta D$ is straightforward, and the method is called the leading edge method [9]. The leading edge method is very computationally inexpensive, but neglects many possible error scenarios. One would have to assume that both sensors receive the same signal, without any difference in atmospheric conditions, and with perfect line of sight. Such conditions are generally not the case in mission scenarios, so more complex methods are employed.

A more robust method is to find the peak of the cross correlation between two received signals. The cross correlation measures the similarity between two signals as a function of time. This cross-correlation enables estimation of the time difference between signals. The equation for determining the time delay $\tau_{delay}$ using the cross correlation is as follows [20]:

$$\tau_{delay} = \arg\max_t \left[(r_1 \star r_2)(t)\right] \tag{2.5}$$

where $r_1$ and $r_2$ are the two received signals, and the $\star$ operator represents the cross correlation operation. This equation assumes a continuous signal, but the process is generally assumed to take place with sampled signals. A sampled signal is one which is digitized by taking discrete samples of a continuous signal such that the characteristics of the original signal are recoverable. An accurate result requires the use of time steps between samples that are small enough to achieve the resolution required for an accurate representation of the original signal. The required resolution for localization purposes depends on the distance between the sensors, the range to the target, and the bandwidth of

the signal of interest (SOI). Resolution is especially important in space based systems because the range is so long.

In practice, to obtain the time difference of arrival through cross correlation, a Fourier transform is performed on each of the received signals, then the conjugate of one signal is multiplied with the other [21]. By doing so, the cross spectral density (CSD) of the two signals is obtained. The CSD is then normalized and the inverse Fourier transform is computed. The resulting vector will have a maximum at the sample associated with the time difference of arrival between the two sensors. The sampling rate $\Delta t$ is known, so the TDOA can be calculated using the difference in sample numbers. Normal practice involves finding the TDOA associated with a common sensor - i.e., have one sensor serve as the basis for all TDOA measurements across the network. The method employed provides $N - 1$ TDOA measurements.

Another way to establish the cross correlation between two signals is the Cross Ambiguity Function (CAF) [21]. The CAF is the method used in this research because the DPD algorithm relies upon this calculation. Avoiding the duplication of effort in this case reduces computation time. The peak magnitude of the CAF matrix is a maximum likelihood estimate for the TDOA [16]. Stein provides the following equation for the CAF $R(\tau, f_d)$ [21]:

$$R(\tau, f_d) = \left| \frac{1}{T} \int r_1^*(f - f_d) r_2(f) e^{-j2\pi f \tau} df \right| \tag{2.6}$$

where $T$ is the collection time span, $f_d$ is the Doppler shift, $\tau$ is the time delay, and the $*$ represents the complex conjugate.

Other approaches are available and well documented, and typically involve a grid search or a Taylor Series expansion [5]. These approaches may require less processing, but are not guaranteed to converge, and may require some initialization.

#### *2.3.1.2 Direction Finding Systems.*

Multiple bearing measurements of passive direction-finding sensors can be combined by a direction finding system to produce an estimate of transmitter position. Once directions are determined from at least two sensors, the LOBs are propagated and the solution is indicated by the point in space where these two (or more) lines cross. As with hyperbolic location systems, noise limits the accuracy of this method. Two dimensional position estimation is often called triangulation. The following equation defines how to determine a LOB estimate, $\theta_i$ from sensor to transmitter, neglecting noise [5]:

$$\theta_i = cos^{-1}\left[\frac{x_t - x_i}{\sqrt{(x_t - x_i)^2 + (y_t - y_i)^2 + (z_t - z_i)^2}}\right],\ 0 \leq \theta_i \leq \pi \tag{2.7}$$

where $[x_t, y_t, z_t]^T$ are the transmitter's coordinates and $[x_i, y_i, z_i]^T$ are the $i^{th}$ sensor's coordinates. It's apparent that $\theta_i$ has an ambiguity such that the quadrant cannot be derived outright. Knowledge of the environment and the target's approximate location can be applied to eliminate the ambiguity. For example, a satellite looking at Earth can eliminate two quadrants altogether by focusing on the two quadrants where the Earth resides.

#### *2.3.1.3 Phase Interferometry.*

Phase interferometry is a method for determining the angle of arrival by measuring the phase difference of an incoming signal between two or more antennas [22]. If both the distance between antennas and the carrier frequency of the incoming signal are known, the phase relationship of the received signals can be determined and the angle of arrival becomes apparent. Figure 2.5 shows the general principle of phase interferometry. This method may provide very accurate results with well tuned hardware and appropriate signal sampling frequencies. However, the accuracy is not without some drawbacks. Phase interferometry requires at least two antennas, and this will only provide about 120 degrees field of view [22]. In order to attain a full 360 degree field of view, along with both azimuth and elevation information, a minimum of four antennas are required [22]. An additional problem with using phase interferometry exclusively results from receiving

multiple signals arriving from different angles. In order to mitigate some of the issues with using phase interferometry, the MUSIC algorithm is employed for this research.

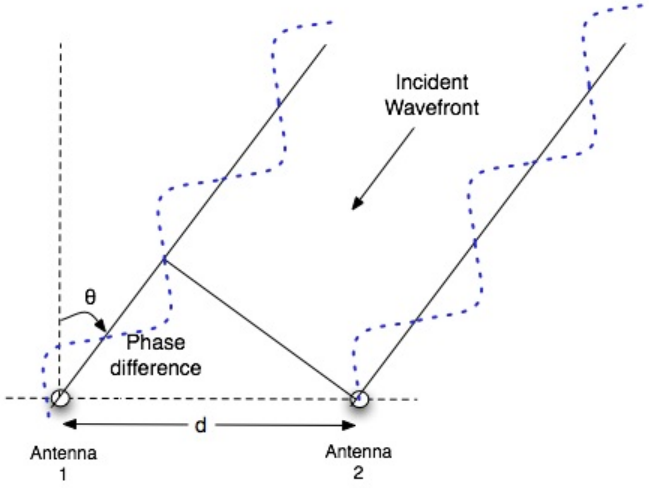


Figure 2.5: Phase Interferometry measures the phase difference between multiple antennas when a plane wave hits the array.

#### *2.3.1.4 The MUSIC Algorithm.*

The MUSIC algorithm is a common technique in direction finding applications [23] - [25]. The technique uses the covariance matrix obtained from $M$ signals received by an antenna array to determine the angle at which the signals arrived. The basic signal model, $\mathbf{x}(t)$, is as follows [26]:

$$\mathbf{x}(t) = \mathbf{A}\mathbf{s}(t) + \mathbf{w}(t) \tag{2.8}$$

where $\mathbf{x}(t)$ is of length $L$, equal to the number of receiving antennas. $\mathbf{A}$ is a vector of $M$ steering vectors, $\mathbf{a}(\theta)$, $\mathbf{s}(t)$ is an $M \times 1$ vector of the source signals, and $\mathbf{w}(t)$ is an $L \times 1$

noise vector. The steering vector $\mathbf{a}(\theta)$ is defined as follows [26]:

$$\mathbf{a}(\theta) = \begin{bmatrix} 1 \\ e^{-j\omega\frac{d\sin\theta}{c}} \\ \vdots \\ e^{-j\omega\frac{(L-1)d\sin\theta}{c}} \end{bmatrix} \tag{2.9}$$

where $\omega$ is the frequency, $d$ is the distance between antenna array elements, and $c$ is the speed of light. In order to use (2.8), the correlation matrix $\mathbf{R_x}$ must be defined [26]:

$$\mathbf{R_x} = E\{\mathbf{x}(t)\mathbf{x}^H(t)\} = \mathbf{A}\mathbf{R_s}\mathbf{A}^H + E\{\mathbf{w}(t)\mathbf{w}^H(t)\} \tag{2.10}$$

where $\mathbf{R_s} = E\left\{\mathbf{s}(t)\mathbf{s}^H(t)\right\} = diag\left\{\sigma_1^2, \ldots, \sigma_L^2\right\}$, the variance of the signal at each receiver. The special case where the elements of the noise vector $w$ are mean zero, variance $\sigma_0$, changes the value of $E\left\{\mathbf{w}(t)\mathbf{w}^H(t)\right\}$ to $\sigma_0^2\mathbf{I}$ [26]. So long as $L > M$, the matrix $\mathbf{A}\mathbf{R_s}\mathbf{A}^H$ is singular. Since $\det\left[\mathbf{A}\mathbf{R_s}\mathbf{A}^H\right]$ is 0, $\sigma_0^2$ must be an eigenvalue of the correlation matrix $\mathbf{R_x}$. In order to execute this procedure, first find the eigenvalues and eigenvectors of the $L \times L$ correlation matrix, then partition them into two sections. The first are the eigenvectors associated with non-zero valued eigenvalues, called $\mathbf{U}_s$. The second section consists of the eigenvectors associated with zero eigenvalues, called $\mathbf{U}_n$. The eigenvectors $\mathbf{U}_s$ and $\mathbf{U}_n$ represent the signal subspace and the noise subspace, respectively, and are represented as follows [26]:

$$\begin{bmatrix} \mathbf{U}_s & \mathbf{U}_n \end{bmatrix} = \begin{bmatrix} u_1 & \ldots & u_M & u_{M+1} & \ldots & u_L \end{bmatrix} \tag{2.11}$$

where $M$ is the number of unique signals that are being received.

The steering vector defined in (2.9) is in the signal subspace, which by definition is orthogonal to the noise subspace. It is therefore known that $\mathbf{a}^H(\theta)\mathbf{U_n} = 0$. If a search through all possible angles from 0° to 90° is performed, the pseudo spatial spectrum in which the correct AOA lies can be mapped. The following equation for the pseudo

spectrum $P(\theta)$ is then used [26]:

$$P(\theta) = \frac{1}{\|\mathbf{a}^H(\theta)\mathbf{U_n}\|^2} \tag{2.12}$$

where $\mathbf{U_n}$ is a matrix of noise subspace eigenvectors. Wherever there exists a peak in $P(\theta)$, there also lies a potential AOA for the arriving signal. For 3D estimates, this procedure must be completed for both azimuth and elevation.

#### *2.3.2 Classical Step 2: Lateration/Angulation Techniques.*

Once the results from each sensor's calculations are complete, they can be sent to a central node for further processing. For most methods, the goal of the second step is to find the places where lines or hyperbolas cross, representing potential transmitter locations. Ideally, all lines will cross at a single point, but with the presence of noise in real-world systems, this is not the case. At the central node, an estimate for the emitter's location in the presence of noise is formed by way of a best fit approach, generally either Maximum Likelihood Estimation (MLE) or Least Squares Estimation (LSE) techniques.

##### *2.3.2.1 Maximum Likelihood Estimation.*

Position estimation in the presence of noise requires the use of a statistical model rather than the deterministic equation it would be in the absence of noise. A set of sensors which obtains $N_s$ samples of the signal will yield $N_s$ position estimates, each of which have some uncertainty associated with them. The MLE method uses the inherently limited number of samples to determine the parameters which maximize the parameters of the likelihood function, and minimize the uncertainty. Casella and Berger give the following definition of MLE [27]:

> For each sample point $\mathbf{x}$, let $\hat{\theta}(\mathbf{x})$ be a parameter value at which $L(\theta|\mathbf{x})$ attains its maximum value as a function of $\theta$, with $\mathbf{x}$ held fixed. A *maximum likelihood estimator* (MLE) of the parameter $\theta$ based on a sample $\mathbf{X}$ is $\hat{\theta}(\mathbf{X})$.

The solution to an MLE problem is typically found by finding the instances when the derivative of the likelihood function is zero. The derivative will provide a maximum, minimum, or point of inflection. A second derivative can provide further information to define the maximum or minimum of the function. In cases when multiple maxima are available, such as when there are multiple satellites with differing position estimates, the global maximum is used.

#### *2.3.2.2 Least Squares Estimation.*

The LSE technique is used in geolocation systems with overdetermined solutions, i.e. a solution with more equations than unknowns. For example, a system using a constellation of five satellites to estimate a three-dimensional location is overdetermined because only four satellites are required. The LSE method can be used to reduce error in the estimate by computing a solution that minimizes the sum of the squared residual terms in a set of range estimates. The LSE technique is commonly used in AOA methods where LOBs are aggregated over a period of time or for an overdetermined set of sensors. To complete the least squares calculations, the quantities $u_i$, $A$, and $b$ are defined [28]:

$$u_i = \frac{v_i - w_i}{\|v_i - w_i\|} \tag{2.13a}$$

$$A = \sum_{i=1}^{N} \mathbf{I} - u_i u_i^T \tag{2.13b}$$

$$b = \sum_{i=1}^{N} \left(\mathbf{I} - u_i u_i^T\right) w_i \tag{2.13c}$$

where $v_i$ is the $i^{th}$ LOB start point's coordinates, $w_i$ is the $i^{th}$ LOB end point's coordinates, and $\mathbf{I}$ is the identity matrix. Using the definitions in (2.13) the minimum error solution can be determined. The least squares estimate of the target's position through AOA estimation is the solution to the equation $x = A^{-1}b$.

### *2.3.3 Closed Form Solution.*

Ho and Chan have developed a closed-form solution to the TDOA based geolocation problem, and address the issues that arise with linearization and iterative methodologies

(such as those proposed by Torrieri [5]). The study concerns the use of geostationary satellites for positioning because geostationary satellites are motionless with respect to a point on the Earth, which reduces error. The solution described uses the geocentric coordinate system. TDOA for each satellite pair is defined as the time from origin at which the correlation function attains the largest value. The solution for the range between the transmitter an the $i^{th}$ receiver, $r_i$, proposed by Torrieri requires linearization using Taylor Series expansion, shown by the following equation [5]:

$$r_i = \sqrt{(x_i - x_t)^2 + (y_i - y_t)^2 + (z_i - z_t)^2},\ i = 1, 2, ..., N \tag{2.14}$$

where $N$ is the number of satellites. The Taylor Series expansion method requires a reasonable initial estimate to converge (convergence is not guaranteed), and is typically processed iteratively. It is also limited to critically determined systems, so extra measurements are discarded. Ho and Chan's method is typically used with four-sensor arrangements, but may be expanded to systems with only three sensors.

#### *2.3.3.1 Four Sensor TDOA Localization.*

A geolocation system using four sensors is capable of producing a three dimensional estimate of the target's position for each time instant that the sensors collectively capture the SOI. Four sensors can yield position computations making use of three equations with three unknowns, so these equations are solved to obtain the emitter's 3D position. Ho and Chan [8] have developed a closed form method for finding the target's position. Kulumani subsequently streamlined this method [29]. The algorithm is summarized in the following discussion.

The relationship $\Delta r_{i,1}$ between the time difference and the Euclidean range difference between a pair of receivers is given as follows [8]:

$$\Delta r_{i,1} = c\tau_{i,1} = r_i - r_1,\ i = 2, 3, 4 \tag{2.15}$$

where $\tau_{i,1}$ is the time delay between sensor $i$ and sensor 1, and $r_i$ is the Euclidean range from the target to the $i^{\text{th}}$ sensor. By inserting the Euclidean range equation into (2.15), the three equations of interest are written with respect to the common sensor's position, $[x_1, y_1, z_1]^T$ [8]:

$$\Delta r_{i,1} = \sqrt{(x_t - x_i)^2 + (y_t - y_i)^2 + (z_t - z_i)^2} - \sqrt{(x_t - x_1)^2 + (y_t - y_1)^2 + (z_t - z_1)^2} \quad (2.16)$$

Squaring both sides of (2.16) and expanding yields the following equation [29]:

$$\Delta r_{i,1}^2 = r_i^2 - 2\Delta r_{i,1} r_1 - r_1^2, \quad i = 2, 3, 4 \quad (2.17)$$

Further simplification as well as putting the equations into matrix form and with respect to the variable $r_1$ yields the following equations [29]:

$$\begin{bmatrix} \Delta r_{2,1}^2 \\ \Delta r_{3,1}^2 \\ \Delta r_{4,1}^2 \end{bmatrix} + 2r_1 \begin{bmatrix} \Delta r_{2,1} \\ \Delta r_{3,1} \\ \Delta r_{4,1} \end{bmatrix} = -2 \begin{bmatrix} x_{2,1} & y_{2,1} & z_{2,1} \\ x_{3,1} & y_{3,1} & z_{3,1} \\ x_{4,1} & y_{4,1} & z_{4,1} \end{bmatrix} \begin{bmatrix} x_t \\ y_t \\ z_t \end{bmatrix} + \begin{bmatrix} K_2 \\ K_3 \\ K_4 \end{bmatrix} - \begin{bmatrix} K_1 \\ K_1 \\ K_1 \end{bmatrix} \quad (2.18)$$

where $K_i = x_i^2 + y_i^2 + z_i^2, \quad i = 1, 2, 3, 4$. The only unknowns in (2.18) are the range from the transmitter to the common sensor, $r_1$, and the transmitter's coordinates, $[x_t\ y_t\ z_t]^T$. In order to find the range $r_1$, the following equations are used to define the temporary vectors $\alpha, \beta$ and the values $A$, $B$, and $C$ [29]:

$$\begin{bmatrix} \alpha_1 \\ \alpha_2 \\ \alpha_3 \end{bmatrix} = - \begin{bmatrix} x_{2,1} & y_{2,1} & z_{2,1} \\ x_{3,1} & y_{3,1} & z_{3,1} \\ x_{4,1} & y_{4,1} & z_{4,1} \end{bmatrix}^{-1} \begin{bmatrix} \Delta r_{2,1} \\ \Delta r_{3,1} \\ \Delta r_{4,1} \end{bmatrix} \quad (2.19)$$

$$\begin{bmatrix} \beta_1 \\ \beta_2 \\ \beta_3 \end{bmatrix} = - \begin{bmatrix} x_{2,1} & y_{2,1} & z_{2,1} \\ x_{3,1} & y_{3,1} & z_{3,1} \\ x_{4,1} & y_{4,1} & z_{4,1} \end{bmatrix}^{-1} \frac{1}{2} \begin{bmatrix} \Delta r_{2,1}^2 - K_2 + K_1 \\ \Delta r_{3,1}^2 - K_3 + K_1 \\ \Delta r_{4,1}^2 - K_4 + K_1 \end{bmatrix} \quad (2.20)$$

$$A = \alpha_1^2 + \alpha_2^2 + \alpha_3^2 - 1 \quad (2.21)$$

$$B = 2(\alpha_1\beta_1 + \alpha_2\beta_2 + \alpha_3\beta_3 - x_1\alpha_1 - y_1\alpha_2 - z_1\alpha_3) \tag{2.22}$$

$$C = K_1 - 2x_1\beta_1 - 2y_1\beta_2 - 2z_1\beta_3 + \beta_1^2 + \beta_2^2 + \beta_3^2 \tag{2.23}$$

These quantities can be put into a polynomial equation as follows [29]:

$$0 = Ar_1^2 + Br_1 + C \tag{2.24}$$

The roots of (2.24) represent the possible values of $r_1$. There will be multiple roots, and the correct one must be chosen for use in (2.18) to obtain the correct transmitter position. A common constraint, which is used in this development, is that the final solution must be a position on or near the Earth's surface. After the roots of (2.24) are input for the $r_1$ term, (2.18) is rearranged to solve for the transmitter position as follows:

$$\begin{bmatrix} x_t \\ y_t \\ z_t \end{bmatrix} = -\begin{bmatrix} x_{2,1} & y_{2,1} & z_{2,1} \\ x_{3,1} & y_{3,1} & z_{3,1} \\ x_{4,1} & y_{4,1} & z_{4,1} \end{bmatrix}^{-1} \left[ \begin{bmatrix} \Delta r_{2,1} \\ \Delta r_{3,1} \\ \Delta r_{4,1} \end{bmatrix} r_1 + \frac{1}{2} \begin{bmatrix} r_{2,1}^2 - K_2 + K_1 \\ r_{3,1}^2 - K_3 + K_1 \\ r_{4,1}^2 - K_4 + K_1 \end{bmatrix} \right] \tag{2.25}$$

The four satellite TDOA solution proposed by Ho and Chan [8] and streamlined by Kulumani [29] can be shown to be a good estimator for geolocation purposes. This algorithm is employed for the research in this thesis.

#### *2.3.3.2 Three Sensor TDOA Localization.*

When only three sensors are available, the TDOA method is still possible, but a constraint is required to determine the transmitter's position. The constraint that the transmitter is on the Earth's surface is again employed, but with only three sensors this constraint will take a much larger role than in Section 2.3.3.1.

The equation for the chief constraint is as follows [29]:

$$r_e^2 = x_t^2 + y_t^2 + z_t^2 \tag{2.26}$$

where $[x_t, y_t, z_t]$ are the coordinates of the transmitter in the Earth-centered Earth-fixed (ECEF) coordinate frame. Reusing (2.17) and the previously defined value of $K_i$,

equations are placed in matrix form in terms of $r_1$ as follows [29]:

$$\begin{bmatrix} x_t \\ y_t \\ z_t \end{bmatrix} = -\frac{1}{2} \begin{bmatrix} x_1 & y_1 & z_1 \\ x_2 & y_2 & z_2 \\ x_3 & y_3 & z_3 \end{bmatrix}^{-1} \begin{bmatrix} K_1 + r_e^2 - r_1^2 \\ K_2 + r_e^2 - r_1^2 - 2\Delta r_{2,1} r_1 - \Delta r_{2,1}^2 \\ K_3 + r_e^2 - r_1^2 - 2\Delta r_{3,1} r_1 - \Delta r_{3,1}^2 \end{bmatrix} \tag{2.27}$$

where $[x_i y_i z_i]$ represents the coordinates of the $i^{th}$ satellite. Notice in (2.27) that $r_e$ plays a significant role in the emitter position solution, in contrast with (2.18), which does not involve $r_e$ at all. The following definitions for the temporary variables $\alpha$, $\beta$, $\gamma$, $a_{ij}$, and **A** through **I** aid in solving for the range from the satellite to the transmitter [29]:

$$\begin{bmatrix} \alpha \\ \beta \\ \gamma \end{bmatrix} = \begin{bmatrix} K_1 + r_e^2 \\ K_2 + r_e^2 - \Delta r_{2,1}^2 \\ K_3 + r_e^2 - \Delta r_{3,1}^2 \end{bmatrix} \tag{2.28}$$

$$\begin{bmatrix} a_{11} & a_{12} & a_{13} \\ a_{21} & a_{22} & a_{23} \\ a_{31} & a_{32} & a_{33} \end{bmatrix} = \frac{1}{2} \begin{bmatrix} x_1 & y_1 & z_1 \\ x_2 & y_2 & z_2 \\ x_3 & y_3 & z_3 \end{bmatrix}^{-1} \tag{2.29}$$

$$\begin{bmatrix} \mathbf{A} \\ \mathbf{D} \\ \mathbf{G} \end{bmatrix} = \begin{bmatrix} a_{11} & a_{12} & a_{13} \\ a_{21} & a_{22} & a_{23} \\ a_{31} & a_{32} & a_{33} \end{bmatrix} \begin{bmatrix} -1 \\ -1 \\ -1 \end{bmatrix} \tag{2.30}$$

$$\begin{bmatrix} \mathbf{B} \\ \mathbf{E} \\ \mathbf{H} \end{bmatrix} = \begin{bmatrix} a_{12} & a_{13} \\ a_{22} & a_{23} \\ a_{32} & a_{33} \end{bmatrix} \begin{bmatrix} -2\Delta r_{2,1} \\ -2\Delta r_{3,1} \end{bmatrix} \tag{2.31}$$

$$\begin{bmatrix} \mathbf{C} \\ \mathbf{F} \\ \mathbf{I} \end{bmatrix} = \begin{bmatrix} a_{11} & a_{12} & a_{13} \\ a_{21} & a_{22} & a_{23} \\ a_{31} & a_{32} & a_{33} \end{bmatrix} \begin{bmatrix} \alpha \\ \beta \\ \gamma \end{bmatrix} \tag{2.32}$$

The values defined in (2.28) - (2.32) can be combined to form a quartic polynomial with respect to $r_1$, as follows [29]:

$$0 = \tilde{A}r_1^4 + \tilde{B}r_1^3 + \tilde{C}r_1^2 + \tilde{D}r_1 + \tilde{E} \tag{2.33}$$

where

$$\tilde{A} = \mathbf{A}^2 + \mathbf{D}^2 + \mathbf{G}^2 \tag{2.34a}$$

$$\tilde{B} = 2\mathbf{AB} + 2\mathbf{DE} + 2\mathbf{GH} \tag{2.34b}$$

$$\tilde{C} = -2x_1\mathbf{A} - 2y_1\mathbf{D} - 2z_1\mathbf{G} + 2\mathbf{AC} + 2\mathbf{DF} + 2\mathbf{GI} + \mathbf{B}^2 + \mathbf{E}^2 + \mathbf{H}^2 - 1 \tag{2.34c}$$

$$\tilde{D} = -2x_1\mathbf{B} - 2y_1\mathbf{E} - 2z_1\mathbf{H} + 2\mathbf{BC} + 2\mathbf{EF} + 2\mathbf{HI} \tag{2.34d}$$

$$\tilde{E} = -2x_1\mathbf{C} - 2y_1\mathbf{F} - 2z_1\mathbf{I} + \mathbf{C}^2 + \mathbf{F}^2 + \mathbf{I}^2 + K_1 \tag{2.34e}$$

The roots of (2.33) are then obtained. There will be four roots, which are the possible ranges from the transmitter to the common sensor. Only two of the four roots will be positive, and the negative roots can be ignored. The two positive roots are substituted back into (2.27) to determine the two possible emitter positions. Additional logic can be applied to determine the root which corresponds to the emitter's position, such as comparison of the solution with the received TOA's to determine the correct solution. However, care must be taken to ensure that the root chosen is on or near the surface of the Earth at the given latitude.

### *2.3.4 Single Step Approach.*

The DPD algorithm takes a different approach to solving for position with a set of receivers. Weiss and Amar [18], along with Pourhomayoun and Fowler [16], show that although each TDOA/FDOA estimate is optimal within each stage of estimation, the two-stage approach itself is not optimal. Error is introduced by not relating each measurement to a single sensor. By processing all of the signals together at a common node this error is eliminated.

The DPD method transforms the sampled received signals into the frequency domain by way of a Fast Fourier Transform (FFT) to separate the time shift from the frequency shift. The resulting signal, $\hat{\mathbf{s}}_n$ is observed as follows [18]:

$$\hat{\mathbf{s}}_n = \alpha_n e^{j2\pi f_d t_{k-1}} \hat{s}(t_k) + w_n(t_{k-1}) \quad \text{for } k \in (0, 1, \ldots, N_s) \tag{2.35}$$

where $\hat{\mathbf{s}}_n$ is $N_s$ samples of the received signals at the $n^{th}$ sensor, $\alpha_n$ is a complex attenuation factor, $f_d$ is the Doppler shift, $\hat{s}$ is the transmitted signal, and $w_l$ is a white Gaussian noise associated with the $n^{th}$ sensor. A grid of possible transmitter positions is created by mapping the sensor response to 2-D grid locations in the matrix $\mathbf{V}_{\mathbf{p_i}}$ using the following equation [16]:

$$\mathbf{V}_{\mathbf{p_i}} \triangleq [\mathbf{D}_1^H \mathbf{W}_1^H \hat{\mathbf{s}}_v^H, \mathbf{D}_2^H \mathbf{W}_2^H \hat{\mathbf{s}}_2^H, \ldots, \mathbf{D}_N^H \mathbf{W}_N^H \hat{\mathbf{s}}_N^H] \tag{2.36}$$

where $\mathbf{D}_1^H$ is the shift operator, $\mathbf{W}_1^H$ is a matrix with $w(t)$ values on the diagonal, and $\hat{\mathbf{s}}_1^H$ is a column vector of received signal samples. In order to find the position estimate, an $N \times N$ matrix $\mathbf{Q}_{p_i} = \mathbf{V}_{p_i}^H \mathbf{V}_{p_i}$ must be calculated for each position on the grid. An exhaustive search is carried out through the grid of potential emitter locations. The point on the grid where $\mathbf{Q}_{p_i}$ attains a global maximum eigenvalue is the position estimate.

Pourhomayoun and Fowler [16] expand on this method by simplifying and distributing it. The original DPD is computationally expensive and requires one sensor to perform the estimation calculations. By approximating the eigenvalue calculations, using Gershgorin's Theorem [30], the DPD method becomes much more attractive for real-world applications. Stein shows that a signal can be decomposed into its TDOA and FDOA components by way of the Complex Ambiguity Function [31]. Pourhomayoun notes that the $\mathbf{Q}_{p_i}$ matrix derived in Weiss' work is merely a grid of individual CAF measurements between sensors. In order to distribute the workload of the algorithm, each sensor can sample the received signal and then transmit those samples to the entire sensor network. Each sensor then computes a CAF matrix for every other sensor in the network and map the matrices to the grid described previously. In order to reduce the

computational load of computing an eigenvalue for each point on the grid, a number of approximations and simplifications can be made.

First, a Gershgorin Disc is used to approximate the eigenvalue [16]. A Gershgorin Disc is an eigenvalue approximation which approximates the eigenvalues of a matrix as the diagonal elements of a row plus or minus an uncertainty term defined by the absolute value of the other elements in that row or column, whichever has a smaller absolute sum. An example using the arbitrary matrix **A** follows:

$$\mathbf{A} = \begin{bmatrix} 5 & 2 & -0.6 & 0 \\ -0.5 & 3 & 0 & 1.4 \\ 0 & 0.8 & 10 & -3 \\ 0.9 & -0.5 & 0 & -12 \end{bmatrix}$$

**A** has Gershgorin Discs $D(5, 1.4)$, $D(3, 1.9)$, $D(10, 0.6)$, $D(-12, 1.4)$. The first and third discs use the column values, while the second and fourth discs use the row values. Gershgorin's Theorem states that every eigenvalue in matrix **A** is located within one of the Gershgorin Discs [30]. If the uncertainty term is sufficiently small, this theorem can be used in determining eigenvalues without the computational load normally required. The eigenvalues in this example are $\lambda_1 = 4.3435$, $\lambda_2 = 3.5749$, $\lambda_3 = 10.0207$, $\lambda_4 = -11.939$.

Using Gershgorin's Theorem in conjunction with knowledge of the grid structure of the CAF allows further simplification [16]. The $\mathbf{Q}_{p_i}$ matrix is Hermitian and positive definite [16], so the columns and rows are conjugates of each other. There is therefore no need to determine whether the column or the row will offer the smallest uncertainty. Now, all each sensor must do is compute the CAFs in relation to the other sensors, find the largest value, and compare it to the other sensors for a final position estimate. Pourhomayoun and Fowler performed a multitude of simulations [16] with results that are near the same quality as the original DPD approach, and exhibit less position estimate error than classical methods (TDOA) in low SNR environments.

### *2.3.5 Instantaneous Received Frequency Approach.*

Nelson and McMahon present a method for geolocating an emitter when its signal is observed by a single moving receiver [19]. The method begins by defining the equation for the instantaneous observed frequency, $\omega^{obs}(t)$ [19]:

$$\omega^{obs}(t) = \omega\left(1 - \frac{v_r(t)}{c}\right) \tag{2.37}$$

where $\omega$ is the transmitted frequency and $v_r(t)$ is the velocity component between the receiver and transmitter. Then, a grid of potential emitter locations $\mathbf{x}$ is constructed. The relative velocity $v_r$ for the receiver is calculated for each point on the grid. The estimated instantaneous received frequency $\omega^{est}(t, \mathbf{x})$ for each of these grid points is calculated as follows [19]:

$$\omega^{est}(t, \mathbf{x}) = \frac{\omega^{obs}(t)}{1 - \frac{v_r(t,\mathbf{x})}{c}} \tag{2.38}$$

The authors suggest two possible ways to estimate the emitter position using $\omega^{est}$. The first method calculates the estimated IRF for each grid point, then determines the grid point with the smallest variance $V$, according to the following equation [19]:

$$V(x) = var_t\left(\omega^{est}(t, \mathbf{x})\right) \tag{2.39}$$

The second method seeks to minimize a cost function, $\mathbf{G}$ which compares $\omega^{obs}$ with the expected received frequency, $\omega^{est}$ from each grid point. The equation for $\mathbf{G}$ is as follows [19]:

$$\mathbf{G}(\mathbf{x}, \Omega) = \int \left(\omega^{obs}(t) - \Omega\left(1 - \frac{v_r(t, \mathbf{x})}{c}\right)\right)^2 dt \tag{2.40}$$

where $\Omega$ is the center frequency of the signal. Conducting an exhaustive search to determine the minimum in either (2.39) or (2.40) among all the grid points provides the estimated transmitter position for the IRF method. Employing an exhaustive search will ensure a global minimum is found.

## 2.4 Sources of Error and Mitigation

The accuracy of a geolocation solution is dependent on three major factors: the accuracy of the sensor's position, the accuracy of range/angle estimates, and the geometric configuration of the sensors and the unknown transmitter position [4]. The first consideration, the accuracy with which the sensor's position is known, is directly related to the positioning knowledge of the Cubesat. The precision of the range and angle estimates is a function of the accuracy of the geolocation model employed, and is the chief concern of the system design. The geometry of the sensors and the transmitter will be a concern due to position dilution of precision (PDOP). PDOP is a unitless measure of a positioning system's geometry with respect to the range between the transmitters and receivers. A good PDOP is a low value, with a minimum of one, and a poor PDOP has a high value.

### *2.4.1 The Importance of Sensor Position Knowledge.*

Accurate position knowledge of a geolocation sensor is crucial in lowering the error of the geolocation estimate. A distinction should be made between position knowledge and position control. A satellite's ability to know precisely its position and attitude is more important to the geolocation solution than its ability to control precisely its position and attitude. From 500 km away, a line of bearing that is off by 2° will cause a position estimate error of 17.5 km [32]. This error can be compounded by poor geometry and timing issues as well. It is therefore prudent to introduce a method to take position knowledge error into account when calculating geolocation estimates. Ho *et al.* provide an algorithm to address the problem of RF source localization in the presence of random receiver location errors [33]. Ho's proposed mitigation method has two stages. First, linearize the geolocation equations (TDOA is used, though expansion to other algorithms is straightforward) with the introduction of a bias parameter related to the receiver location. Next, use the induced bias to refine the emitter location estimate through the use of a weighted least squares minimization using the range values computed in the first

stage. Some assumptions are made along the way in the derivation. First, it is assumed that the measurement noise in the sensor is independent of the receiver location noise. Also, the algorithm requires knowledge of the covariance matrices from the measurements and from the receiver locations. These values would require some calibration via in-orbit testing with a signal at a known location. The result of the study was the derivation of the increase in the Cramer-Rao Lower Bound (CRLB), and an algebraic solution to improve the estimation accuracy in the presence of receiver position knowledge uncertainty was found to meet this new CRLB.

### *2.4.2 Range and Angle Estimate Accuracy.*

The precision of range and angle estimation is largely a function of the quality of data collected by the sensors and the accuracy with which a system can analyze that data. The sensors in this research will be in space, 450 km above the Earth's surface. In order for a signal to reach the satellite's antenna, it must have enough power to travel that distance and still stand out from the noise. An antenna with a suitable gain pattern is essential to detecting the target signals when they are not designed for communication with the sensors.

Most geolocation algorithms rely on an accurate timing system to determine the time a signal arrives at a sensor in order to calculate either a distance measurement or a LOB. Cubesats generally don't have the space available for a clock that is more accurate than a crystal oscillator, so the timing for geolocation related measurements must be taken from larger satellites nearby (most likely GPS satellites). Allan notes that "...every clock disagrees with every other clock essentially always, and no clock keeps ideal, or 'true' time in an abstract sense except as we may choose to define it" [34]. Allan discusses the variables which are prone to error in all timing systems, such as frequency drift, frequency offset, time offset, and random deviations. All of these variables can be aggregated into a

clock error term, which is unavoidable in localization systems. A typical clock error in Cubesats that rely on GPS is on the order of 40 ns [35].

### *2.4.3 Additional Error Sources.*

Additional sources of error include multipath, NLOS, and atmospheric factors. Multipath refers to the propensity of electromagnetic waves to reflect off of objects present in the path between the transmitter and the sensor. Multipath causes multiple replicas of the signal to be received at the sensor over time, often with delayed signals attenuated due to the absorption of energy during the reflection. The effects of multipath include uncertainty in determining which received signal is the original LOS signal, as well as the deterioration of signal strength and structure. Another scenario in which multipath is an issue is when there is no LOS signal received. In this case, there is an object blocking the line of sight, so only the multipath signals arrive at the sensor, causing a bias in the range estimate. An important measure of the effect of multipath on a system's ability to resolve multipath channels is the bandwidth [4]. As bandwidth is increased, the time domain resolution is increased, which improves range estimates [4]. Narrowband systems are therefore degraded more severely than wideband systems. A model of multipath signal $h$ delayed by $\tau$ is as follows [4]:

$$h(\tau) = \sum_{k=1}^{L_p} \alpha_k e^{j\phi_k} \delta(t - \tau_k) \tag{2.41}$$

where $L_p$ is the number of multipath channels, and the quantities $\alpha_k$, $\phi_k$, and $\tau_k$ are the amplitude, phase, and propagation delay of the $k^{th}$ path, respectively.

Another error to be concerned with is atmospheric attenuation. The angle at which the signal passes through the upper atmosphere may have an effect on the speed at which the signal travels and may diffract the signal as it travels through the channel. There are many models that deal with elements of atmospheric attenuation. Barts [36] and Panagopoulos [37] model the propagation of high frequency satellite communication waves. Wang and Sarabandi [38] examine wave propagation through foliage. Rain can

degrade signals in the K band as well, leading to severe attenuation of the signals by the time they arrive at the sensors. The effects of atmospheric attenuation will not be a focus of this research. Another factor which affects the attenuation of a signal when propagated through the atmosphere is the signal's frequency. A higher frequency signal, such as one in the X band, will attenuate differently through the atmosphere than a lower frequency signal such as one in the VHF/UHF band. A system's target frequency can have an effect on the design of several aspects of the system as well.

#### *2.4.4 The Effect of Frequency.*

Transmitter frequency is an important consideration in a geolocation system. A signal's carrier frequency can limit the effective range of communication, the receiver antenna array design, the range between receivers, and many other factors which go into the design of the geolocation system. Airborne receivers typically have the space to carry multiple antenna arrays to perform a wide range of missions with different frequency requirements. A small space-borne system is much more limited in both space available for antenna arrays and the ability to change hardware with each new mission. The frequency and beamwidth of the signal may influence the spacing of the satellites as well, and would then affect the PDOP. Sensors that are closer to each other in position yield a higher PDOP, which will degrade performance.

Another concern is how the antenna's gain pattern affects geolocation capabilities. At lower frequencies, there is not much of an issue because it is easier to build antennas which have a good omnidirectional gain pattern. However, as frequency increases it becomes more difficult to maintain a high gain in a variety of directions [39]. The front end of the sensor platform must have a well engineered antenna array which provides a gain pattern suitable for the specific mission.

## 2.5 Performance Measures

There are many ways in which geolocation methods can be analyzed and measured to compare their performance. Some methods rely on statistical means to measure the lower variance bounds on the solution. Other methods evaluate the geometry of the problem space for information about how well the geolocation methods might work. A simple method to gauge performance of an estimator is to run many iterations of a simulation and track the average error over the ensemble.

### *2.5.1 Cramer Rao Lower Bound.*

The CRLB is a statistical lower bound on the variance of an unbiased estimator [40]. Comparing results using the CRLB provides insight into the effectiveness of a particular algorithm, and can aid in the detection of biases and inefficiencies. The CRLB is a function of several factors, chief among them the number and geometry of the sensors, the measurement type, and the dimension of the solution space (i.e. 2D or 3D).

At the heart of the CRLB is the Fisher Information Matrix (FIM). The FIM measures the amount of information that a random variable $\mathbf{X}$ holds in relation to an unknown parameter $\theta$, according to the following equation [41]:

$$FIM(\theta) = -\mathrm{E}\left\{\frac{\partial^2 ln\left(p\left(\mathbf{X};\theta\right)\right)}{\partial\theta^2}\right\} \tag{2.42}$$

The expected value of the second derivative of the signal's probability distribution function (PDF) provides the FIM for each independent observation. Another useful feature of the FIM is that each observation's FIM can be added together to assess arrays of signal samples, so long as the observations are independent.

In a general case, this research assumes that the distribution of the noise summed with the signal is Gaussian, and so has the following PDF, $p(\mathbf{X};\theta)$ [41]:

$$p(\mathbf{X};\theta) = \frac{1}{\left(2\pi\sigma^2\right)^{N_s/2}} exp\left(\frac{-1}{2\sigma^2}\sum_{n=0}^{N_s-1}\left(X[n] - s_r[n;\theta]\right)^2\right) \tag{2.43}$$

where $\sigma^2$ is the variance of each observation, $N_s$ is the number of samples collected, $X$ is the received signal, and $s_r$ is the transmitted signal. Taking the natural logarithm then differentiating (2.43) twice with respect to the variable of interest $\theta$ results in the following equation [41]:

$$\frac{\partial^2}{\partial\theta^2}\ln p(\mathbf{X};\theta) = \frac{-\sum_{n=0}^{N_s-1}\left[\frac{\partial s_r[n;\theta]}{\partial\theta}\right]^2}{\sigma^2} \tag{2.44}$$

In order to find the CRLB, the result of (2.44) is inverted as follows [41]:

$$var(\hat{\theta}) \geq \frac{\sigma^2}{\sum_{n=0}^{N_s-1}\left[\frac{\partial s_r[n;\theta]}{\partial\theta}\right]^2} \tag{2.45}$$

The generalized CRLB formula in (2.44) and (2.45) will change based on the relationship between $s_r$ and $\theta$.

### *2.5.2 Dilution of Precision (DOP).*

An important factor to consider in geolocation accuracy is the geometry between the satellites and the transmitter. A large intersection angle is desirable [8], and increasing the distance between satellites is helpful for this. There is a limit to how far apart the sensors can be positioned before performance is degraded. Ho and Chan provide a set of equations that can be used to determine this limit [8]. Also, there is a balance that should be considered between the PDOP and the target transmitter's beamwidth. In order to maximize the SNR, satellites must remain within one beamwidth of the transmitting antenna. The transmitter's beamwidth is a concern in designing the orbit used in transmitter detection. Some applications cannot assume a known transmitter beamwidth and transmitter bearing, and would need to keep the range between the satellites small to ensure that the signal is collected by all of the sensors simultaneously. The scenario necessitates a poor dilution of precision in order to meet the required signal collection parameters for the geolocation algorithms to run.

PDOP is a concern in all localization methods, but can be much more pronounced in far-field applications. The relative distance between a sensor and the transmitter is

generally much greater than the distance between the sensors, which makes the various range estimates from sensors to transmitter very close numerically. PDOP is calculated by a root-sum-square of the autocorrelation values of distance measurements in the sensor's relation to the transmitter. The PDOP equation is as follows [42]:

$$PDOP = \sqrt{\sigma_x^2 + \sigma_y^2 + \sigma_z^2} \tag{2.46}$$

where $\sigma_x$, $\sigma_y$, and $\sigma_z$ represent position uncertainty in their respective coordinate directions. These values, referred to as "sigma values", increase as the range measurements between sensors increase in correlation. Larger sigma values yield more diluted position estimates due to increased overlap in noisy range estimates. Figure 2.6 shows examples of both good and poor PDOP.

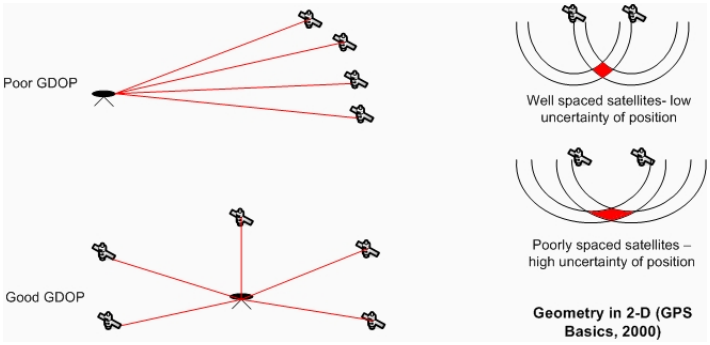


Figure 2.6: Poor PDOP can increase uncertainty in the positioning accuracy of geolocation systems, while good PDOP can lessen the uncertainty [43].

## 2.6 Cubesat Characteristics

The Cubesat standard is a relatively recent development in the satellite community. In the 1990's, many satellite programs began designing increasingly large and complex satellites which were envisioned to save money by doing many missions onboard rather than just one. Many programs, however, found that the increased complexity of the

platform actually led to more problems, more delays, and more cost [32]. More complex missions, combined with the ever-shrinking microprocessor, led to a new trend to simplify and miniaturize satellites. Smaller and cheaper was perceived as better, and thus a standard was created. The Cubesat is a satellite standard started by Puig-Suari and Twiggs at Cal Poly and Stanford in 1999 [44]. The base platform size is 10 x 10 x 10 $cm^3$ and weighs no more than 1.33 kg - this is called 1U (One Unit). For the past decade, Cubesats have been primarily used for university research projects due to their small payload and affordability. Educational, military, and commercial interest has grown substantially as their demonstrated capabilities have expanded.

The advantages of using satellites to perform a geolocation mission stem from their vantage point from orbit. The field of view is much greater than what could be achieved by an airborne platform. Additionally, there are advantages in policy, as there are no overfly restrictions for satellites. The likelihood of a satellite being forcibly removed from service are low as well, so a satellite is a resilient host for the geolocation mission.

The idea of developing space-based assets on a short timeframe and a small budget has been a popular topic in recent years. The ORS Office has the following task [45]:

> ...plan and prepare for the rapid development of highly responsive space capabilities that enable delivery of timely warfighting effects and, when directed, develop and support deployment and operations of these capabilities to enhance and assure support to Joint Force Commanders′ and other users′ needs for on-demand space support, augmentation, and reconstitution.

Cubesats may be an excellent way to to effectively and efficiently provide reconnaissance and intelligence to warfighters on the short timeline desired by ORS. The use of Cubesats specifically for this type of mission is beneficial because of their cost effectiveness and relatively short design and build time. The low cost of production for a Cubesat could allow a set of satellites to be built and placed on the shelf for short-notice surveillance

requirements. The time-to-launch factor of a solution like this is then limited only by the time required to determine an optimal orbit and RF front end, then launch. The ORS timeline goal of months to a year [45] is feasible.

## 2.7 Cubesat Capabilities

Selva and Krejci [32] give a good introduction to the capabilities and limiting factors of Cubesats used in an Earth observation mission. One such limiting factor is the capability for data transmission, which is much more restrictive than the capability for data storage. A typical Cubesat has a downlink data rate of 0.25 Mbps, and only has about 5 minutes of access to the ground station per pass. The short access window leads to a maximum transmission capability of 9.3 MB per pass, far below the gigabytes of data storage that may be available [32]. The difference could affect the geolocation mission if a large amount of data is required to be post-processed at the ground station. The amount of computation that can be performed on-board the satellite can mitigate the need to transmit extensive data back to the ground station, but at the cost of power, computation time, and required on-board storage.

Another limiting factor which has an immediate implication for geolocation algorithm accuracy is the attitude determination sensors. Current technology has achieved accuracies of less than 2° on a deployed satellite (CanX-2) [32]. This system uses sun sensors and magnetometers for attitude awareness. A star-tracker could be employed with better results, but there doesn't appear to be an operational Cubesat with such a system in place [32]. There are currently star trackers in development which would achieve attitude measurement accuracy of 0.5° [32]. This accuracy would lower position uncertainty on the ground to 4.5 km from 17.5 km for a 2° position knowledge accuracy.

The dimensions of the Cubesats also present some limitations. There are obvious difficulties that come with a small payload, to include less computational ability, less robust communication, and shorter lifespan. Receiver capability can be degraded as well.

The maximum diameter of an RF antenna on a 1U Cubesat is 10 cm, which corresponds to the wavelength of a 3 GHz signal. Any fixed antenna put on-board the 1U Cubesat will not be a full wavelength for signals below the C-band. The length restriction could affect gain and SNR of the antenna, and may reduce communication or sensing capabilities. Deployable antennae can be included in the payload, but this increases the risk of mechanical failure and impacts the space available for other hardware on-board the Cubesat. This research focuses on a 6U Cubesat architecture, which will lessen the effect of such limitations. A 6U Cubesat has a maximum of 30 cm length for a fixed antenna, allowing communications in the L-band.

## 2.8 Geolocation System Designs

The state of the art in geolocation systems is evolving to include satellites as a sensor platform. There are a number of satellite systems which have been designed to perform a geolocation mission. The Satelllite Mission for Swarming and Geolocation (SAMSON) project is a three-Cubesat constellation mission concept designed to perform autonomous cluster flight and geolocation of a cooperative RF emitter on the surface of Earth [46]. The SAMSON project is led by the Technion (the Isreali Institute of Technology) and supported by the Israeli space industry. As of this writing, SAMSON is in the design phase, with anticipated launch in 2015. The satellite swarm will use TDOA and FDOA to perform a geolocation estimate for use in search and rescue operations. The system is intended for a 'lost at sea' scenario where a transmitting wristband will be worn by boaters to provide the satellites *a priori* information of the signal structure. The geolocation system is expected to determine TDOA measurements within 100 nanoseconds and FDOA measurements within 0.5 Hertz. Knowledge of satellite orientation and position is expected to be within 0.5 degrees of truth using a combination of Earth and Sun sensors, magnetometers, and magnetorquers.

Although Cubesats are beginning to see more interest for geolocation missions, larger satellites are predominantly used. A recent patent from Northrop Grumman Systems Corporation shows a design for an interferometer based geolocation system. The satellite would carry an interferometer array to produce a set of direction of arrival vectors [47]. The system would only require a single satellite to perform the methods proposed in the patent. Qualcomm Incorporated have proposed a similar application, where two satellites are used to determine the position of a user. The patent filed by Levanon *et al.* uses TDOA and FDOA to perform geolocation to locate a cooperative signal source.

## 2.9 Summary

This section presented a background of the geolocation problem and its solution methods. There are two primary classical methods which have been developed to support the research into localization methods. TDOA uses the difference in reception times between sensors to estimate the source of an RF transmission. AOA methods calculate lines of bearing from the receivers to create a position estimate based on where those LOBs cross. Another classical method, FDOA, is often used to supplement TDOA or AOA with frequency difference measurements if the receivers and/or the transmitters are moving. DPD is a new localization method which uses a cost function for a single step solution. DPD has been shown to significantly improve geolocation performance in systems with a low SNR. The research with respect to the DPD method has been focused on a geolocation problem measured in tens of kilometers. Research into the performance of the DPD method at standoff distances of hundreds or thousands of kilometers is unique to this research, and is explored in this thesis.

Cubesats are a relatively new platform in the satellite community. Small in size and budget, they are ideal for programs where the mission is computationally inexpensive and design time is short. In a scenario where information about a target C3 node is needed on short notice, Cubesats can be deployed quickly if there is a model in place to determine

the best solution for a particular set of parameters. A pre-built Cubesat constellation could be uploaded with the appropriate algorithms in software and deployed with little preparation time.

# III. Methodology

This chapter provides the reader with a detailed description of the simulations conducted and the algorithms used in this work. The simulation environment is described, to include the transmitter characteristics, signal of interest parameters, and methods used to geolocate. The performance metrics used to evaluate the various geolocation methods are detailed as well.

## 3.1 Problem Overview

The problem considered is the geolocation of a fixed RF transmitter with a variable number of Cubesats in LEO above the target. The satellites are capable of receiving the signal while in orbit, and are able to communicate with other satellites in the constellation to share the gathered information about the received signal. The satellites are in radio communication with a ground station or a network of ground stations to communicate location estimates and error parameters to the user. Figure 3.1 depicts an anticipated mission scenario.

## 3.2 Simulating the Space Environment

In order to simulate the space environment in the scenario, care has be taken to ensure the space-borne sensors are modeled as moving according to realistic orbit parameters. Also, the simulation of the signal must be modeled realistically in its propagation through free-space from the transmitter's position to the satellites' positions. The satellites are modeled to be in constant motion along their orbits, so a Doppler shift is simulated and associated with the signal as well.

The AGI System Tool Kit (STK) is used in this research to simulate the satellites' positions throughout their orbits. STK is a tool commonly used by astronautical engineers and satellite designers to build realistic scenarios involving spacecraft, heavenly bodies,

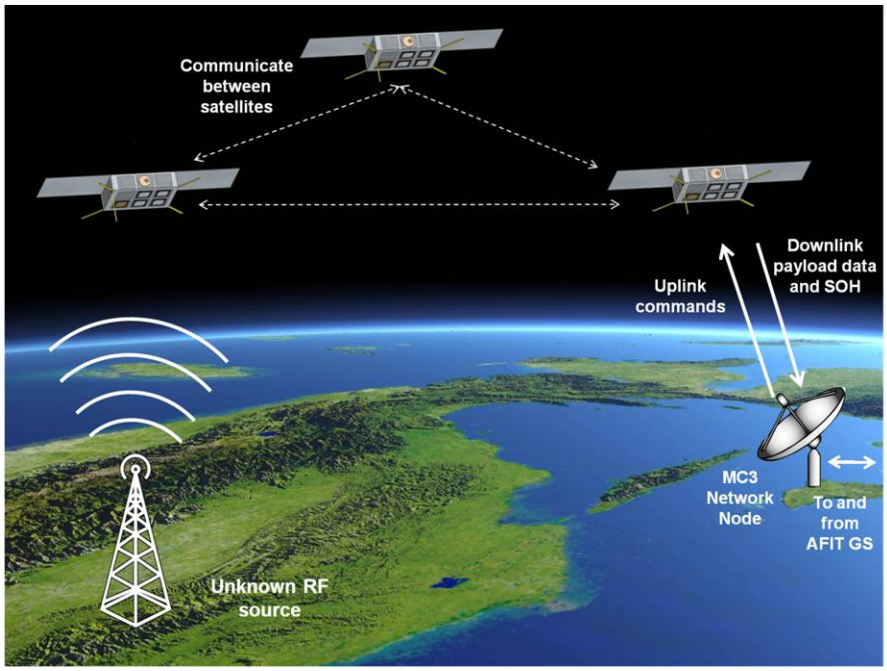


Figure 3.1: Scenario Overview

and Earth-based objects. The tool allows for simulation of communication connections between satellites and sensors on the ground, and is able to accurately determine the position of each satellite when the communication link is available. This data can be exported from STK and then be imported into Matlab for use in the geolocation simulation.

In a real world scenario, the orbit parameters would be chosen to fit the mission - i.e. to maximize time over target, number of passes per day, etc. For this research, the site of the simulated transmitter is chosen to be AFIT, at the geodetic coordinates [39.782272° N -84.082893° W 0]. The altitude of 0 meters indicates that the transmitter is on the surface of the Earth.

Table 3.1 shows the orbit parameters for a four satellite scenario. When multiple satellites are simulated, the inclination angle is changed by 0.5°, and the altitude is increased by 1 km for each additional satellite to reduce the risk of collision in orbit. The

Table 3.1: Orbit Parameters

| | Cubesat 1 | Cubesat 2 | Cubesat 3 | Cubesat 4 |
|---|---|---|---|---|
| Altitude | 450 km | 451 km | 452 km | 453 km |
| Eccentricity | 0° | 0° | 0° | 0° |
| Inclination | 50° | 49.5° | 49° | 50.5° |
| Period | 93.6 minutes | 93.6 minutes | 93.6 minutes | 93.6 minutes |
| Maximum Pass Time | 10 minutes | 10 minutes | 10 minutes | 10 minutes |

details of the orbit parameter trade space are not the focus of this research, but they are chosen to increase time-over-target and improve constellation geometry while over the target. While over the target, the geometry changes from a point with one satellite to a line with two satellites, a triangle shape with three satellites, or a parallelogram shape with four. The PDOP for these formations is better than that offered by a straight line formation. Figure 3.2 illustrates the scenario from Table 3.1, with four satellites orbiting over the target in three dimensions in STK.

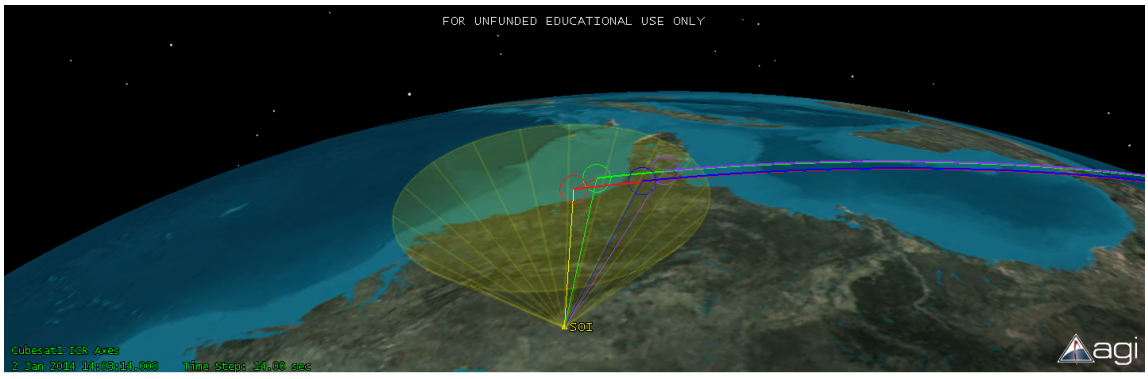


Figure 3.2: 3D Orbit Over Target

The simulation considered in this research only uses a single pass over the target to generate the geolocation estimate. The Cubesats receive the signal for 515 seconds along the orbit, and each second the satellite positions are updated according to the orbital information generated by STK. Figure 3.3 shows the considered orbit over the target. The pass used in this research does not pass directly over the target, nor is it the longest pass possible. In realistic scenarios, it would be unlikely to pass directly over the target, as its position is unknown. The closest point in the satellite's trajectory is approximately 770 km from the target.

Figure 3.3: The portion of the orbit considered in this research does not pass directly over the target. The red star represents the target and the colored asterisks represent the Cubesat positions over time.

## 3.3 System Parameters

The geolocation system is comprised of $N$ satellites. The composition of the constellation is varied. The satellite is modeled as having four antennas with associated

receiver radios on-board each of the satellites, and the radios are able to receive the SOI and accurately detect frequency and phase information. Reference timing on a Cubesat is typically based on GPS because there is not enough space for a finely calibrated oscillator on-board. There are some small oscillators available, such as the Symmetricom Quantum [48] and the Jackson Labs CSAC [49]. The difficulty with including these oscillators is that they would necessitate synchronization between sensors, which adds further error potential and requires more power. For this research, therefore, it is assumed that GPS timing is used, and that the timing has a Gaussian error with mean zero and a standard deviation of 40 nanoseconds [35].

Once the signal is received, sampled, and filtered, it can be sent to the on-board processor. This research assumes that the geolocation algorithms are executed on-board the satellite. With the sampled signal available, the processor can extract the information required to perform geolocation. As discussed in Section 2.1, this may include information about timing, phase, frequency, or some combination of all of these. The satellite then transfers the extracted data to a central node. From there, data are compiled and an estimate is computed. The estimate may be output to the ground station, saved in memory for tracking purposes, or both. In addition to the position estimate, an estimate of the solution's variance can be determined. The combination of the estimate and its variance provides the user with insight into where to search for the target. Figure 3.4 shows an overview of the processing flow from signal reception to final position estimate.

## 3.4 Models for Signal Generation, Transmission, and Reception

The signal produced by the transmitter is assumed to be a narrowband signal, transmitted with enough power to remain above the noise floor when received at LEO. The bandwidth of the narrowband signal is approximately 100 kHz. The waveform generated in the simulation is a 50 microsecond square pulse, as shown in Figure 3.5.

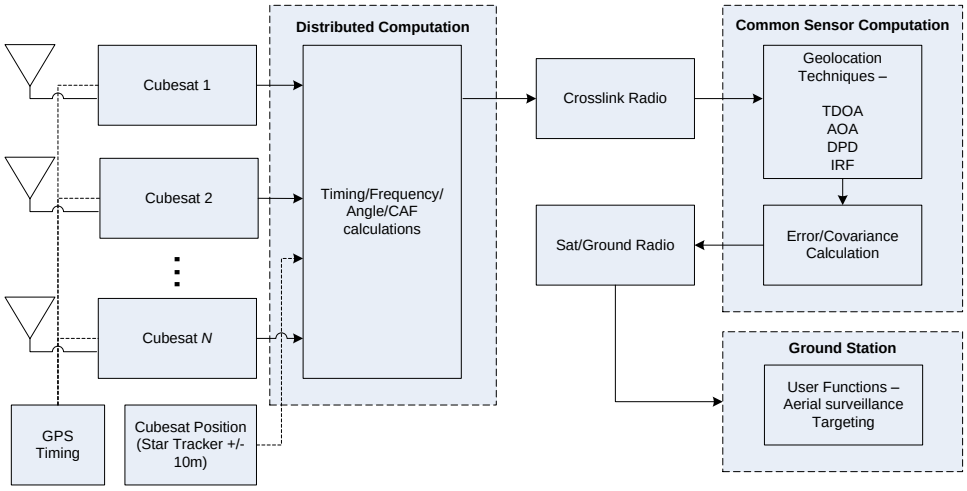


Figure 3.4: Processing Flow

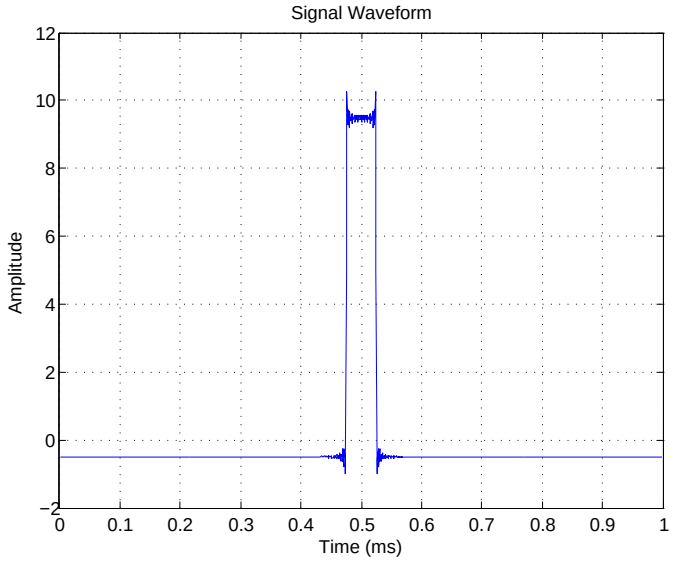


Figure 3.5: Simulated Transmission Signal

The signal can be broadcast with varying power, which changes the quality of the received signal. The simulated transmission signal is comprised of 500 sinusoids added

together to form a square pulse. The equation used in the simulation to model the transmission signal $s(t)$ is the following:

$$s(t) = \sum_{n=1}^{500} a_n cos\left(2\pi n f_c t\right) \tag{3.1}$$

where $a_n$ is the amplitude, $f_c$ is the carrier frequency of the signal, and $t$ is the time vector. For a square pulse, the amplitude is a sinc function, which is modeled as follows:

$$a_n = \frac{2A \sin\left(2\pi n \frac{k}{T}\right)}{2\pi n} \tag{3.2}$$

where $A$ is the amplitude of the pulse, $k$ is the width of the pulse, and $T$ is the period. To model channel effects as the signal is broadcast, $s(t)$ is delayed by $\tau$, shifted by the Doppler frequency $f_d$, and attenuated by $\alpha$, yielding the signal $r(t)$. The received signal is modeled as follows:

$$r(t) = \alpha \left[\sum_{n=1}^{500} a_n cos\left(2\pi n f_c \left(t - \tau\right)\right)\right] e^{j2\pi f_d t} + w(t) \tag{3.3}$$

where a noise term $w(t)$ is included in $r(t)$ to simulate additive white Gaussian noise (AWGN) that would be present in the received signal. The received signal can vary widely depending on the variables inserted into (3.3). The noise added to the signal is of a magnitude dictated by the SNR at the receiver. A signal with a large SNR may be from a powerful radar system, while a signal with a small SNR may be attributed to a smaller Earth-based communication system.

The time shift $\tau$ that is applied to the signal corresponds with the time delay associated with LOS signal propagation. It is assumed in this research that the signal propagates at $c = 2.9978 \times 10^8$ m/s. A signal traveling directly from the transmitter to the Cubesat directly overhead at an altitude of 450 km is assumed to have a time delay $\tau$ of 1.5 milliseconds.

The Doppler shift corresponds with the velocity of the satellite relative to the transmitter. The typical speed of a satellite in LEO is on the order of 7,500 m/s. This

yields a substantial Doppler shift which can be measured to provide information about the emitter's position. The speed is related to the position of the receiver as well as the timing of the samples. The Cubesat orbit position error is generally less than 10 meters when using an on-board star tracker [50]. A Gaussian error with mean zero and a standard deviation of 10 meters is added to each receiver position to simulate these errors. Using the equation for Doppler shift for a stationary transmitter and a moving observer, the Doppler shifted frequency $f_d$ is as follows:

$$f_d = \left(\frac{c + v_r}{c}\right) f_c \tag{3.4}$$

where $v_r$ is the satellite's velocity relative to the transmitter and $f_c$ is the carrier frequency of the transmitted signal. If the satellite is moving toward the transmitter, the relative velocity will be positive and $f_d$ will be larger than $f_c$. If the satellite is moving away from the transmitter, the relative velocity will be negative and $f_d$ will be smaller than $f_c$.

It should be noted that atmospheric conditions may change some of the signal propagation parameters, such as the speed and path loss of the propagated signal. Applying a more robust model for atmospheric conditions will improve the accuracy of the simulations, but accounting for atmospheric attenuation characteristics is not in the scope of this research. Accounting for these characteristics is an area for further research.

## 3.5 Algorithms

Four algorithms are considered in this research for the estimation of transmitter position. Two classical methods - TDOA and AOA - are implemented along with a version of the DPD method and the IRF method. These algorithms were developed in Chapter II. The following sections will detail their use in the simulations built for this research.

### *3.5.1 Time Difference of Arrival.*

Chapter II describes the overall goal of the TDOA method - to extract meaningful timing information from a signal and use that information to obtain the difference in time

of arrival between a group of sensors. Once the TDOA information is extracted, a multilateration algorithm follows to obtain a position estimate. A closed form multilateration approach formulated by Ho and Chan [8] is used in this research. The algorithm is developed as presented by Kulumani [29], and as described in Sections 2.3.3.1 to 2.3.3.2. The closed form approach is chosen because it will always converge, though it may be more computationally burdensome.

An important change to Kulumani's method must be implemented in this simulation. Kulumani based his calculations on a spherical Earth, and this simulation uses an elliptical Earth model, the WGS coordinate system, to determine the positions of the transmitter and sensors. The radius of the Earth which is used in (2.26) must be modified, or else the resulting emitter position will have a significant source of error built into the equation. This error will increase as the transmitter is moved away from the equator, so the error is maximized when the transmitter is located at one of the Earth's poles. It is prudent, therefore, to determine the approximate Earth radius at the latitude of the transmitter. In practice, the latitude may not be implicitly known. If a general target area is known (such as if it is known that the transmitter is located near a certain city), the latitude could be approximated by the user. If the target whereabouts are completely unknown, the process could be conducted iteratively, where Earth's equatorial radius is used first and then the latitude is refined after the estimate is computed. This research assumes that the transmitter is known to be in or near a large city, whose approximate latitude is known. The equation to find the radius of the Earth $r_e(\psi)$ at a given geodetic latitude is the following [51]:

$$r_e(\psi) = \sqrt{\frac{(a^2 \cos\psi)^2 + (b^2 \sin\psi)^2}{(a \cos\psi)^2 + (b \sin\psi)^2}} \tag{3.5}$$

where $\psi$ is the geodetic latitude of the transmitter, $a$ is the Earth's equatorial radius (6378 km), and $b$ is the Earth's polar radius (6356 km). Using the calculated value of $r_e$ from 3.5 should reduce a significant error source, relative to that which would be found when using

Kulumani's method. The TDOA method can only be used when three or more satellites are available in the geolocation system.

### *3.5.2 Angle of Arrival.*

The angle of arrival is calculated using the MUSIC algorithm, which was developed in Section 2.3.1.4. Simulations associated with this research assume a single signal is present, even though the MUSIC algorithm is applicable in multi-signal environments (provided there are more antennas than the number of signals present). The satellite is simulated to have an antenna array consisting of two antennas per direction estimated. Azimuth and elevation angles are required to construct a three dimensional line of bearing. Once the bearing angles are estimated, the line of bearing is calculated beginning at the satellite's coordinates and propagating out in the direction of the emitter. LOB's are defined using a point of origin (i.e. the satellite's position) and an associated bearing angle. As more LOB's are created, they can be aggregated to find the origin of the signal by determining cross points. There will be multiple points where the lines cross due to noise in the signal. When three LOB's are present in 2D this will create a 'cocked hat', as described by Stein [31].

This research presumes a 3D coordinate system, which makes the process of finding crossings in LOB's more complicated. A LOB in 3D has an origin point and two associated angles for azimuth and elevation, $(\theta, \phi)$. Multiple LOB's from noisy signals may never actually intersect in three dimensions. Instead of finding the center of Stein's 'cocked hat', a better approach is to use a least squares method. Least squares essentially finds a position estimate in 3D space which minimizes the distance between that point and each of the 3D LOBs. Least squares is used to obtain the final estimate of the target's position through the AOA method, as described in Section 2.3.2.2.

When three or more sensors are available to geolocate in the simulation, a 3D estimate is created for each time epoch when a measurement is made. When only one or

two satellites are present, the LOBs are aggregated over a period of time, and a least squares estimate is found using (2.13).

### *3.5.3 Position Determination from LOB's.*

Once the LOB's are calculated by the MUSIC algorithm described in Section 2.3.1.4, they are combined with the associated satellite positions to determine the target estimate through least squares approximation. The bearing lines are defined by two points in space - an origin and an end point. The origin is the satellite's position, $v_i = [x_i\ y_i\ z_i]^T$, and the end point $w_i = \left[x_{prop}\ y_{prop}\ z_{prop}\right]$ is found by propagating the angle of arrival out from the satellite's position. The range of propagation should be far enough to ensure the surface of the Earth is surpassed. For this simulation the propagation range $r_{prop}$ is calculated as follows:

$$r_{prop} = 1.5 \times \arg\max_{N}(r_i) \tag{3.6}$$

where $r_i$ is the Euclidean range from the $i^{th}$ satellite to the target.

### *3.5.4 Direct Position Determination.*

The DPD method is based upon classical TDOA and FDOA methods, but formulates emitter positions in a single step rather than the dual steps of calculating timing and Doppler prior to estimating position. The original method proposed by Weiss [18] requires the computations to be done at a single node, and requires a series of CAF's to be computed. Pourhomayoun and Fowler have simplified the computations and distributed the processing in their paper [16]. Weiss' original method is used in this research.

The signal model for Weiss' method is more complex than the signal models used for the TDOA discussion in Section 2.3.1.1. The received signal at the $n^{th}$ sensor $\mathbf{s}_{rn}[m]$ is defined as follows [18]:

$$\mathbf{s}_{rn}[m] = b_n\mathbf{a}_n(\mathbf{p})s_{tn}[m] + \mathbf{w}_n[m], \quad m \in \{0, \ldots, N_s - 1\} \tag{3.7}$$

where $\mathbf{s}_{rn}$ is a $1 \times N_s$ vector, $b_n$ is a complex number representing attenuation, $\mathbf{a}_n(\mathbf{p})$ is the array response at the $n^{th}$ sensor from the transmitter's coordinates $\mathbf{p}$, $s_{tn}$ is the transmitted

signal, $\mathbf{w}_n[m]$ is AWGN, $m$ is the discrete time sample number, and $N_s$ is the number of samples. In order to extract the useful information from the received signal waveform, a discrete Fourier transform (DFT) is performed on the received signal. The frequency domain signal $\bar{\mathbf{s}}_{rn}$ follows [18]:

$$\bar{\mathbf{s}}_{rn}[m] = b_n \mathbf{a}_n(\mathbf{p}) \bar{s}_{tn}[m] e^{-j\omega_m[\tau_n(\mathbf{p})+t_0]} + \bar{\mathbf{w}}_n[m], \quad m \in \{0, \ldots, N_s - 1\} \tag{3.8}$$

where $\bar{\mathbf{s}}_{rn}$ is a $1 \times N_s$ vector, $\omega_m = \frac{2\pi m}{N_s T}$, $k$ is between 0 and $N_s - 1$, $\tau_n(\mathbf{p})$ is the propagation delay, and $t_0$ is the transmit time. To optimize the process, the equation for the cost function $Q(\mathbf{p})$ is minimized as follows [18]:

$$Q(\mathbf{p}) = \sum_{n=1}^{N} \|\bar{\mathbf{s}}_{rn}\|^2 - \sum_{n=1}^{N} \left| \mathbf{a}_n^H(\mathbf{p}) \sum_{k=0}^{N_s-1} e^{j\omega_k[\tau_n(\mathbf{p})+t_0]} \bar{s}_{tn}^*[m] \bar{\mathbf{s}}_{rn}[m] \right|^2 \tag{3.9}$$

The equation for $Q(\mathbf{p})$ is cumbersome, but it can be manipulated by searching for the maximum of the second term rather than the minimum of the entire expression. Searching for the maximum may delete a term in the equation, but there is still an unknown, immeasurable quantity in the equation, $\bar{s}_{tn}^*$. Working under the assumption that the original signal's waveform and transmit time are unknown, this term must be resolved. In order to accomplish this, the vectors $\mathbf{d}_n$ and $\bar{\mathbf{s}}$ are defined as follows [18]:

$$\mathbf{d}_n \equiv [d_n(0), \ldots, d_n(N_s - 1)]^T \tag{3.10a}$$

$$d_n(k) \equiv e^{j\omega_k \tau_n(\mathbf{p})} \mathbf{a}_n^H \bar{\mathbf{s}}_{rn}(k) \tag{3.10b}$$

$$\bar{\mathbf{s}} \equiv [\bar{s}_{tn}(0) e^{-j\omega_0 t_0}, \ldots, \bar{s}_{tn}(N_s - 1) e^{-j\omega_{N_s-1} t_{N_s-1}}] \tag{3.10c}$$

The cost function in (3.9) can then be rewritten as follows [18]:

$$\tilde{Q}(\mathbf{p}) = \sum_{n=1}^{N} |\bar{\mathbf{s}}^H \mathbf{d_n}|^2 \tag{3.11}$$

The transmitted signal $\bar{\mathbf{s}}$ is independent of the sensors, so if a matrix $\mathbf{D}$ is defined as $\mathbf{D} = \sum_{n=1}^{N} \mathbf{d}_n^H \mathbf{d}_n$, $\tilde{Q}(\mathbf{p})$ can be expressed as follows [18]:

$$\tilde{Q}(\mathbf{p}) = \bar{\mathbf{s}}^H \mathbf{D} \bar{\mathbf{s}} \tag{3.12}$$

The vector $\bar{\mathbf{s}}$ is unknown, but it can be assigned to be the eigenvector corresponding to the largest eigenvalue in $\mathbf{D}$. This assignment achieves the maximum of $\tilde{Q}(\mathbf{p})$. The only unknown in (3.12) is $\mathbf{D}$, because $\mathbf{s}$ is a fixed and unknown quantity. Therefore, $\tilde{Q}(\mathbf{p})$ is maximized by defining the vector $\bar{\mathbf{s}}$ as the eigenvector corresponding to the largest eigenvalue of the matrix $\mathbf{D}$, an $N \times N$ matrix [18].

The DPD method relies on a grid search model to provide an estimate for the emitter's position [18]. The literature on the DPD method primarily uses a two dimensional model, leading to a square grid of possible emitter positions. Using satellites requires a three dimensional grid to ascertain the best estimate. The cube begins with 125 points spaced evenly throughout the structure, then adds a random error factor with zero mean and a standard deviation which starts at 100 meters and shrinks to 10 meters as the cube size is decreased. The size of the bounding box is 200 km on each side to start, and is decreased by 20 percent after each iteration until the box is 10 meters on each side.

#### *3.5.5 Instantaneous Received Frequency Method.*

The IRF method uses the changing velocity of the satellite relative to the emitter to approximate the position of the transmitter. As discussed in Section 2.3.5, a grid of possible emitter locations is defined, and estimated instantaneous received frequency is calculated for each grid point.

For this research, the simulation creates a three dimensional cube with the center point at the true emitter position, plus an error factor which is random and less than 100 meters. The grid initially consists of 125 points, or five grids which are each $5 \times 5$, spaced evenly throughout the cube. The size of the bounding box is 200 km on each side to start. Once the estimated IRF is calculated for each point in the cube, the closest match is decided and the next cube is constructed with that point as the center. The dimension of the bounding cube is reduced by 20 percent until the box is 10 meters on each side.

In order to calculate the instantaneous frequency of the received signal, the Welch method is used [52]. The simulation for the IRF method uses a signal of length $N_s = 10,000$ samples, a Hanning window with a length of 1000 samples, and an overlap of 500 samples.

## 3.6 Performance Measurements

The performance metrics used to evaluate the methods examined in this simulation scenario are the Cramer-Rao lower bound (CRLB) and the position dilution of precision (PDOP). These metrics are related, but provide the designer with different information about the target solution that may be useful in design decisions. The generalized CRLB is developed in Section 2.5.1, and is further detailed below according to the various measurement types which are used in this research.

### *3.6.1 Cramer-Rao Lower Bound.*

The CRLB is applied in this research to show how the various methods of geolocation used in the simulation perform relative to the statistical lower bound on the variance of the position estimate. The CRLB is the inverse of the FIM for the collected data, and a convenient form of the FIM for the data $\mathbf{f}(\mathbf{x})$ is as follows [53]:

$$\mathbf{J} = \mathbf{H}^T \mathbf{C}^{-1} \mathbf{H} \tag{3.13}$$

where $\mathbf{H}$ is the Jacobian and $\mathbf{C}$ is the covariance matrix for the collected signal. The Jacobian is calculated according to the positions of the sensors in addition to the parameters of interest. The basic form of the Jacobian $\mathbf{H}$ can be represented as the following [53]:

$$\mathbf{H} \equiv \frac{\partial \mathbf{s}(\mathbf{p})}{\partial \mathbf{p}} = \begin{bmatrix} \frac{\partial s_1(\mathbf{p})}{\partial x_t} & \frac{\partial s_1(\mathbf{p})}{\partial y_t} & \frac{\partial s_1(\mathbf{p})}{\partial z_t} & \frac{\partial s_1(\mathbf{p})}{\partial f_c} \\ \frac{\partial s_2(\mathbf{p})}{\partial x_t} & \frac{\partial s_2(\mathbf{p})}{\partial y_t} & \frac{\partial s_2(\mathbf{p})}{\partial z_t} & \frac{\partial s_2(\mathbf{p})}{\partial f_c} \\ \frac{\partial s_3(\mathbf{p})}{\partial x_t} & \frac{\partial s_3(\mathbf{p})}{\partial y_t} & \frac{\partial s_3(\mathbf{p})}{\partial z_t} & \frac{\partial s_3(\mathbf{p})}{\partial f_c} \\ \frac{\partial s_4(\mathbf{p})}{\partial x_t} & \frac{\partial s_4(\mathbf{p})}{\partial y_t} & \frac{\partial s_4(\mathbf{p})}{\partial z_t} & \frac{\partial s_4(\mathbf{p})}{\partial f_c} \end{bmatrix} \tag{3.14}$$

where $s_1$ - $s_4$ are the equations for the parameters of interest, and $\mathbf{p}$ is the transmitter position and frequency, $\mathbf{p} = [x_t \; y_t \; z_t \; f_c]$. The parameters which are of interest in this research are timing, frequency, and bearing, respectively. Bearing encompasses both azimuth and elevation angles. The equations for $s_1$ - $s_4$ are the following [53], [54]:

$$s_1 = \frac{R_i - R_j}{c} \tag{3.15}$$

$$s_2 = \frac{f_c}{c}\frac{dR_i}{dt} \tag{3.16}$$

$$s_3 = \alpha_{i(az)} + \frac{180}{\pi}\arctan\left(\frac{y_t - y_i}{x_t - x_i}\right) \tag{3.17}$$

$$s_4 = \alpha_{i(el)} + \frac{180}{\pi}\arccos\left(\frac{z_t - z_i}{R_i}\right) \tag{3.18}$$

where $R_i$ is the range to from the $i^{th}$ satellite to the transmitter and $\alpha_i$ is the direction of the antenna main lobe. The number of parameters which are used to calculate the CRLB for position is dependent on the geolocation method being used. For example, when just the DPD method is used, only $s_1$ and $s_2$ are used for timing and frequency information. The elements of the Jacobian in (3.14) can be computed with (3.15) - (3.18) as follows:

$$\frac{\partial s_1(\mathbf{p})}{\partial x_t} = \frac{1}{c}\left(\frac{x_t - x_i}{\sqrt{(x_t - x_i)^2 + (y_t - y_i)^2 + (z_t - z_i)^2}} - \frac{x_t - x_j}{\sqrt{\left(x_t - x_j\right)^2 + \left(y_t - y_j\right)^2 + \left(z_t - z_j\right)^2}}\right)$$

$$\frac{\partial s_1(\mathbf{p})}{\partial y_t} = \frac{1}{c}\left(\frac{y_t - y_i}{\sqrt{(x_t - x_i)^2 + (y_t - y_i)^2 + (z_t - z_i)^2}} - \frac{y_t - y_j}{\sqrt{\left(x_t - x_j\right)^2 + \left(y_t - y_j\right)^2 + \left(z_t - z_j\right)^2}}\right)$$

$$\frac{\partial s_1(\mathbf{p})}{\partial z_t} = \frac{1}{c}\left(\frac{z_t - z_i}{\sqrt{(x_t - x_i)^2 + (y_t - y_i)^2 + (z_t - z_i)^2}} - \frac{z_t - z_j}{\sqrt{\left(x_t - x_j\right)^2 + \left(y_t - y_j\right)^2 + \left(z_t - z_j\right)^2}}\right)$$

$$\frac{\partial s_1(\mathbf{p})}{\partial f_c} = 0$$

$$\frac{\partial s_2(\mathbf{p})}{\partial x_t} = \frac{f_c}{c}\frac{(x_t - x_i)\left(V_x(x_t - x_i) + V_y(y_t - y_i) + V_z(z_t - z_i)\right)}{\left((x_t - x_i)^2 + (y_t - y_i)^2 + (z_t - z_i)^2\right)^{\frac{3}{2}}}$$

$$\frac{\partial s_2(\mathbf{p})}{\partial y_t} = \frac{f_c}{c}\frac{(y_t - y_i)\left(V_x(x_t - x_i) + V_y(y_t - y_i) + V_z(z_t - z_i)\right)}{\left((x_t - x_i)^2 + (y_t - y_i)^2 + (z_t - z_i)^2\right)^{\frac{3}{2}}}$$

$$\frac{\partial s_2(\mathbf{p})}{\partial z_t} = \frac{f_c}{c}\frac{(z_t - z_i)\left(V_x(x_t - x_i) + V_y(y_t - y_i) + V_z(z_t - z_i)\right)}{\left((x_t - x_i)^2 + (y_t - y_i)^2 + (z_t - z_i)^2\right)^{\frac{3}{2}}}$$

$$\frac{\partial s_2(\mathbf{p})}{\partial f_c} = \frac{1}{c}\left(\frac{\left(V_x(x_t - x_i) + V_y(y_t - y_i) + V_z(z_t - z_i)\right)}{\sqrt{(x_t - x_i)^2 + (y_t - y_i)^2 + (z_t - z_i)^2}}\right)$$

$$\frac{\partial s_3(\mathbf{p})}{\partial x_t} = \frac{180}{\pi}\left(\frac{-(y_t - y_i)}{(x_t - x_i)^2 + (y_t - y_i)^2}\right)$$

$$\frac{\partial s_3(\mathbf{p})}{\partial y_t} = \frac{180}{\pi}\left(\frac{(x_t - x_i)}{(x_t - x_i)^2 + (y_t - y_i)^2}\right)$$

$$\frac{\partial s_3(\mathbf{p})}{\partial z_t} = 0$$

$$\frac{\partial s_3(\mathbf{p})}{\partial f_c} = 0$$

$$\frac{\partial s_4(\mathbf{p})}{\partial x_t} = \frac{180}{\pi}\frac{(z_t - z_i)(x_t - x_i)}{\sqrt{1 - \frac{(z_t - z_i)^2}{(x_t - x_i)^2 + (y_t - y_i)^2 + (z_t - z_i)^2}}\left((x_t - x_i)^2 + (y_t - y_i)^2 + (z_t - z_i)^2\right)^{\frac{3}{2}}}$$

$$\frac{\partial s_4(\mathbf{p})}{\partial y_t} = \frac{180}{\pi}\frac{-(z_t - z_i)(y_t - y_i)}{\sqrt{1 - \frac{(z_t - z_i)^2}{(x_t - x_i)^2 + (y_t - y_i)^2 + (z_t - z_i)^2}}\left((x_t - x_i)^2 + (y_t - y_i)^2 + (z_t - z_i)^2\right)^{\frac{3}{2}}}$$

$$\frac{\partial s_4(\mathbf{p})}{\partial z_t} = \frac{180}{\pi}\frac{\frac{1}{\sqrt{(x_t - x_i)^2 + (y_t - y_i)^2 + (z_t - z_i)^2}} - \frac{(z_t - z_i)^2}{\left((x_t - x_i)^2 + (y_t - y_i)^2 + (z_t - z_i)\right)^{\frac{3}{2}}}}{\sqrt{1 - \frac{(z_t - z_i)^2}{(x_t - x_i)^2 + (y_t - y_i)^2 + (z_t - z_i)^2}}}$$

$$\frac{\partial s_4(\mathbf{p})}{\partial f_c} = 0$$

The matrix **C** has the covariances for the parameters of interest along the diagonal, according to the following:

$$\mathbf{C} = \begin{bmatrix} C_1 & 0 & 0 \\ 0 & \ddots & 0 \\ 0 & 0 & C_N \end{bmatrix} \tag{3.19}$$

where $N$ is the number of parameters being used to find the CRLB, and the parameters of interest are assumed to be uncorrelated. The diagonal elements of **C** can be calculated by finding the expected value of the parameter equations according to (3.15) - (3.18) as follows:

$$E[s_1 s_1^*] = \frac{1}{c^2}\left(\text{var}\left(\hat{R}_i\right) + \text{var}\left(\hat{R}_j\right)\right) \tag{3.20}$$

$$E[s_2 s_2^*] = \frac{1}{c^2}\text{var}\left(\hat{f}\right)\frac{dR_i}{dt} \tag{3.21}$$

$$E[s_3 s_3^*] = \alpha_{i(az)} + \frac{180}{\pi}\text{var}\left(\hat{\theta}_{az}\right) \tag{3.22}$$

$$E[s_4 s_4^*] = \alpha_{i(el)} + \frac{180}{\pi}\text{var}\left(\hat{\theta}_{el}\right) \tag{3.23}$$

Once the Jacobian and the covariance matrix are calculated they can be used in the following equation to calculate the CRLB for position estimation:

$$C_{CRLB}(\mathbf{p}) = \mathbf{J}^{-1} = \left[\mathbf{H}^T \mathbf{C}^{-1} \mathbf{H}\right]^{-1} \tag{3.24}$$

The following sections will describe the variances for the individual parameters of interest.

#### *3.6.1.1 Time Delay / Range Measurements CRLB.*

To measure the TDOA position estimation performance, the CRLB for time delay is calculated, then the parameters are changed to measure the range estimator performance. The CRLB $\text{var}(\hat{\tau}_0)$ for time delay is the following [41]:

$$\text{var}(\hat{\tau}_0) \geq \frac{1}{SNR \times B_{rms}^2} \tag{3.25}$$

where $B_{rms}$ is the RMS bandwidth of the received signal. $B_{rms}$ is defined as follows [41]:

$$B_{rms} = \sqrt{\frac{\int_{-\infty}^{\infty} (2\pi f)^2 |S(f)|^2 df}{\int_{-\infty}^{\infty} |S(f)|^2 df}} \tag{3.26}$$

In order to change the CRLB from being defined with respect to $\tau$ to being defined with respect to range, a change of variables is performed such that $R = \frac{c\tau_0}{2}$, and $CRLB_{\hat{R}} = \left(\frac{\partial R}{\partial \tau_0}\right)^2 CRLB_{\hat{\tau}_0}$. After this conversion, the final CRLB var($\hat{R}$) for the range equation is as follows [41]:

$$\text{var}(\hat{R}) \geq \frac{c^2/4}{SNR \times B_{rms}^2} \tag{3.27}$$

#### *3.6.1.2 Bearing Measurements CRLB.*

Assuming that the wavefront is a plane, the scenario is illustrated as shown in Figure 2.5. The sampled signal $\mathbf{X}[n]$ at the $n^{th}$ sensor can be written as follows [53]:

$$\mathbf{X}[n] = A\cos\left(\Omega_s n + \hat{\phi}\right) + w[n] \tag{3.28}$$

where $A$ is the signal's amplitude, $\Omega_s$ is the spatial frequency (rad/sensor), and $\hat{\phi}$ is a phase delay factor. The parameters in (3.28) which will fold into the equation for CRLB are $\theta = [A\ \Omega_s\ \hat{\phi}]^T$. The parameter of interest in this case is the AOA $\beta$, which is a function of $\Omega_s$. The other two parameters are considered nuisance parameters, but must remain in the equations even though they are not the parameter of interest. $\beta$ can be written as follows [53]:

$$\beta = \arccos\left(\frac{c\Omega_s}{2\pi f_0 d}\right) \tag{3.29}$$

where $d$ is the distance between antennas in the receiving array. The Fisher Information Matrix $\mathbf{I}(\theta)$ for this problem is the following [41]:

$$\mathbf{I}(\theta) = \begin{bmatrix} \frac{N}{2\sigma^2} & 0 & 0 \\ 0 & \frac{A^2}{2\sigma^2}\sum_{n=0}^{N_s-1} n^2 & \frac{A^2}{2\sigma^2}\sum_{n=0}^{N_s-1} n \\ 0 & \frac{A^2}{2\sigma^2}\sum_{n=0}^{N_s-1} n & \frac{N_s A^2}{2\sigma^2} \end{bmatrix} \tag{3.30}$$

The variance bound results from the inverse of the Fisher Information Matrix along with the change of variables in (3.29). The CRLB var($\hat{\beta}$) for a direction finding algorithm is bounded as follows [41]:

$$\text{var}(\hat{\beta}) \geq \frac{12}{(2\pi)^2 SNR \times M\frac{M+1}{M-1}\left(\frac{L}{\lambda}\right)^2 \sin^2(\beta)} \tag{3.31}$$

where $M$ is the number of antennas in the receiving antenna array, $L$ is the total length of the array, and $\lambda$ is the wavelength of the signal of interest.

#### *3.6.1.3 Frequency Estimation CRLB.*

The lower bound on the frequency estimation for a collected signal can also be found from the inverse of (3.30), without a change of variable. The lower bound for frequency estimation is the following [41]:

$$\text{var}\left(\hat{f}_0\right) \geq \frac{12}{(2\pi)^2 SNR \times N\left(N^2-1\right)}\left(\text{Hz}^2\right) \tag{3.32}$$

The frequency accuracy decreases as $\frac{1}{N^3}$, so the length of the collected signal has an important impact on the performance of the estimator.

### *3.6.2 Dilution of Precision.*

Dilution of precision measures the quality of the solution with respect to the position of the sensors and the transmitter, as discussed in Section 2.5.2. This research uses PDOP instead of GDOP because timing error found in the GDOP calculations is not considered for the algorithms that are investigated in this research. The DOP is related to the CRLB [40]. If the estimator is efficient, then the relationship between the DOP and the CRLB is var($\theta$) = $\sigma_d PDOP$, where $\sigma_d$ is the variance of the range measurement. The PDOP is important in satellite based geolocation especially because there is a set, predictable orbit which the sensors follow. The orbit is essentially fixed unless the satellites are equipped with enough fuel to perform more than station keeping movement.

## 3.7 Simulation Variables

The primary drivers of the results of the simulator described in this chapter are the variables which modify the environment. This simulation uses four variables to generate emitter position estimates. First, the number of satellites in the geolocation constellation is varied from one to four. This necessitates the use of different algorithms for different configurations. Some algorithms, such as TDOA and DPD, cannot work with a single satellite. Second, the SNR of the received signal is varied from -35 to +35 dB in order to simulate different transmitter power levels. The SNR is the only metric used in this research to measure the quality of the received signal itself. Third, the size of the bounding box applied to the target search grid is varied. This parameter is not applicable in some algorithms, such as AOA. The performance of the algorithms when these variables are changed provides information as to their usefulness in different scenarios, and should aid designers in the creation of effective geolocation systems.

## 3.8 Summary

This chapter has provided the reader with a detailed description of the simulation environment, variables, algorithms, and performance metrics used. The simulator presented makes use of a robust model of the environment in which the geolocation system must operate, and will provide the user with an estimate of the emitter's position for a given set of environmental variables.

Chapter IV showcases the results of simulation, and indicates how the chosen variables will affect the performance of the geolocation system.

# IV. Results and Analysis

This chapter presents analysis of the results of the simulations described in Chapter III. Multiple scenarios are presented, with parameters described and results analyzed and discussed. The performance metrics introduced in Chapter II are analyzed as well, with respect to the scenarios established in this chapter. Section 4.1 introduces the variables common to all of the scenarios presented. Sections 4.2 to 4.5 discuss the scenarios used to determine geolocation performance. Sections 4.6 to 4.9 analyze how some variables will affect the system's geolocation estimate. Section 4.10 summarizes the results from this research.

## 4.1 Global Parameters

The global parameters used in simulation are those which are true for the entire ensemble of scenarios presented in this research. The SNR used in each scenario is varied from -35 dB to +35 dB in 10 dB increments. The orbit parameters noted in Section 3.2 are not changed throughout the scenarios, though each scenario uses a different number of satellites. A total of 515 discrete 1 ms long received signals are used, representing the signal collected during a single pass over the target. Timing errors associated with the satellites' individual 'true' time result from use of the GPS system, and are Gaussian with zero mean and a standard deviation of 40 ns, as described in Section 3.3. The satellite's knowledge of its own position is assumed to be accurate to within 10 meters, which is typical for a satellite using a star tracker to estimate position. The simulated emitter is located at the Air Force Institute of Technology, and is stationary.

## 4.2 Scenario 1 - A Single Satellite

A single satellite relies upon a changing position along its orbit to locate a stationary emitter in three dimensions, as discussed in Section 2.1.1. Simulations for the single

satellite scenario use the AOA and IRF methods. These two methods are employed because they do not require multiple measurements within the same time epoch to solve for the emitter's position.

The position estimate is extrapolated from lines of bearing for the AOA method and a grid search of potential emitter locations for the IRF method, as detailed in Sections 3.5.2 and 3.5.5, respectively. The IRF method measures the Doppler of the received signal over time, and compares the measured frequency to the calculated frequency from each grid point. The true frequency and simulated instantaneous received frequency at an SNR of +5 dB is shown in Figure 4.1. Notice the 'bunching up' of the measurements at the edges of the figure. The satellite's elevation angle, as seen from the transmitter, will change more rapidly as the satellite reaches the closest point to the target along its trajectory overhead.

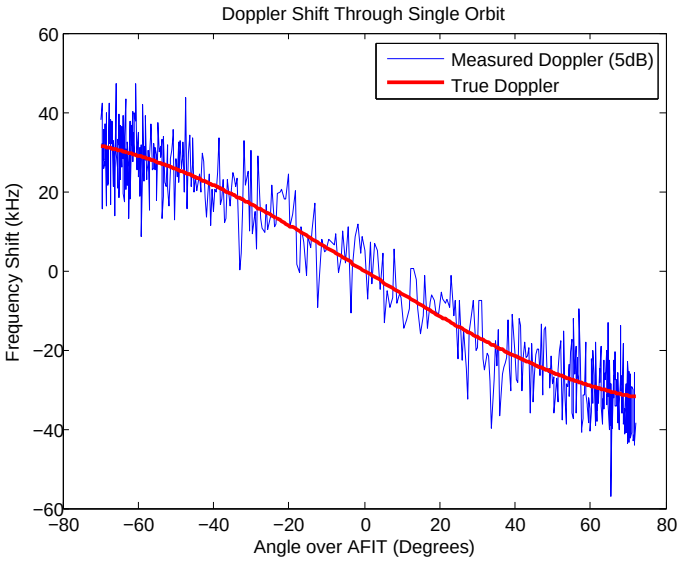


Figure 4.1: True Doppler and Measured Doppler (SNR = +5 dB)

In this scenario, the sensor travels along an orbit according to Table 3.1. The simulation is considered with 20 trials per SNR step. Figure 4.2 shows the modeled performance of the AOA and IRF methods in this scenario.

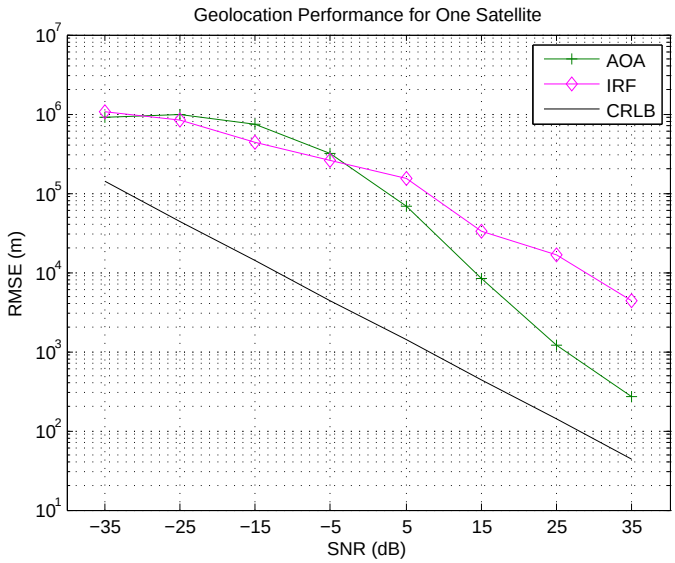


Figure 4.2: Algorithm performance for a single satellite scenario

The IRF method appears to perform better than the AOA method at lower SNR values, and the AOA method's performance begins to diverge from the IRF method's performance when the SNR reaches -5 dB. Both estimators continue to track alongside the CRLB as the simulated signal's SNR increases. However, the AOA method outperforms the IRF method by a wide margin at higher SNR values.

The trade space for a single satellite geolocation system design includes the hardware requirements, data storage and throughput requirements, processing requirements, and performance requirements. A significant difference in the hardware requirements of these two methods is the number of antennas required to perform the relevant measurements. The AOA method requires a minimum of four antennas to achieve a three dimensional bearing estimate $(\theta, \phi)$. More antennas improve the accuracy of the MUSIC estimation algorithm, so the antenna array design for a Cubesat employing the AOA method is an important part of the overall system design. The IRF method requires a single antenna, as the only measurement is of the instantaneous frequency of the received signal. The hardware requirements are not a focus of this research, but are mentioned to give the

reader an idea of the trade space. The IRF method is much more sensitive to the duration of a received signal than the AOA method is, so it will require more data storage and handling. The performance requirements depend greatly on the expected signal strength, hardware available, orbit parameters, and other factors. If the best possible performance is desired, the AOA method will generally perform better than the IRF method. However, if hardware space is limited and a slightly diminished geolocation performance is acceptable, the IRF method may be a better option. The Cubesat architecture is small enough that the value of less or smaller hardware is often higher than the performance of the payload, so the IRF method may be a better option, depending on the circumstances.

### 4.3 Scenario 2 - Two Satellites

Adding a second satellite increases the performance of the geolocation system. A second satellite provides twice the information per time epoch, allowing each method to converge to a solution faster. Although adding a second satellite inevitably induces a time synchronization error between the two satellites, other errors are reduced. Two satellites offer a dimensional aspect to the receivers that was not present with a single satellite. The satellites maintain a distance of approximately 70 km from each other while in the range of the emitter's signal. The angular separation of the two satellites as seen from the transmitter's point of view is at most 9°. While this separation is very small, the slight offset in orbit between the two receivers will provide small differences in the Doppler frequency and angle measurements made by the platforms. These differences help distinguish the closest grid point in the IRF method, and will provide the AOA method with more LOB's to use for its localization process.

In this scenario, the sensors travel along orbits as described in Table 3.1. The simulation was run with 20 trials per SNR step, and converges toward the CRLB as the SNR is increased. Figure 4.3 illustrates the simulated performance of the AOA and IRF methods in this scenario.

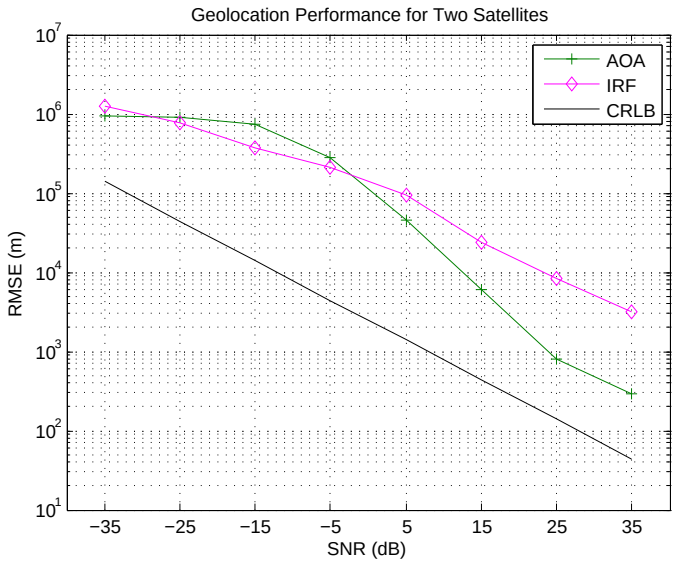


Figure 4.3: Algorithm performance for a dual satellite scenario.

The AOA method performs better than the IRF method at higher SNR values, similar to the single satellite scenario. However, the gap in performance between the two methods is smaller when two satellites are present.

The two satellite scenario must include trade space considerations, similarly to the single satellite scenario, but will add some new conditions. If two satellites are to work cooperatively, a communications link must exist between satellites if any joint processing is to be done on-board. The additional communications hardware will take up space, which contributes to the argument against the larger payload hardware that the AOA method requires. The data that must be transferred between the two sensor platforms is relatively small for each method. The AOA method only requires the transmission of the LOB's calculated and the satellite positions for each time epoch. The IRF method requires the transmission of the measured instantaneous received frequency and the satellite's position for each time epoch. Again, the size of the platform and the good performance of the IRF method may make it a well balanced choice for system designers.

## 4.4 Scenario 3 - Three Satellites

A third satellite enables the use of DPD and TDOA. The DPD method makes use of both time and frequency information, as discussed in Section 3.5.4. TDOA can be performed with the constraint that the emitter's position is on the surface of the Earth, as detailed in Section 2.3.3.2. The AOA and IRF methods are still used in simulations to compare performance, but in this scenario with three measurements per time epoch. A constellation of three satellites will also permit the geometry of the receivers in a triangle formation rather than a line, which is the case when using just two satellites. The triangle geometry improves the geolocation estimate, and the PDOP may now be calculated.

The geometry between three satellites and the transmitter is much improved over having just two satellites. The PDOP improves as the satellites move across the target overhead. Also, the orbit parameters for the third satellite are adjusted in inclination so that the constellation is at its widest while over the target. The PDOP reaches its minimum of 53 when the satellites are directly over the target.

The performance of each of the four algorithms is shown in Figure 4.4. The four algorithms are run in 20 trials over the range of SNR values.

The DPD method outperforms the AOA and IRF methods by more than an order of magnitude for the span of -15 to +15 dB SNR. TDOA nearly matches the performance of DPD above -5 dB SNR, and all methods approach the CRLB as the SNR is increased. The AOA and IRF methods both improve performance with three satellites, but do not match the DPD or TDOA methods in performance. It is interesting to note that the TDOA method outperforms the DPD method at both extremes of the SNR used in the simulation. The bounding box for the DPD method plays a part in the decreased performance at low SNRs. The bounding box for this simulation is 2,000 km per side. The simulation shows that the performance of the DPD method at less than -25 dB is highly dependent on the size of the emitter location grid used in the DPD algorithm. For high SNR, the TDOA

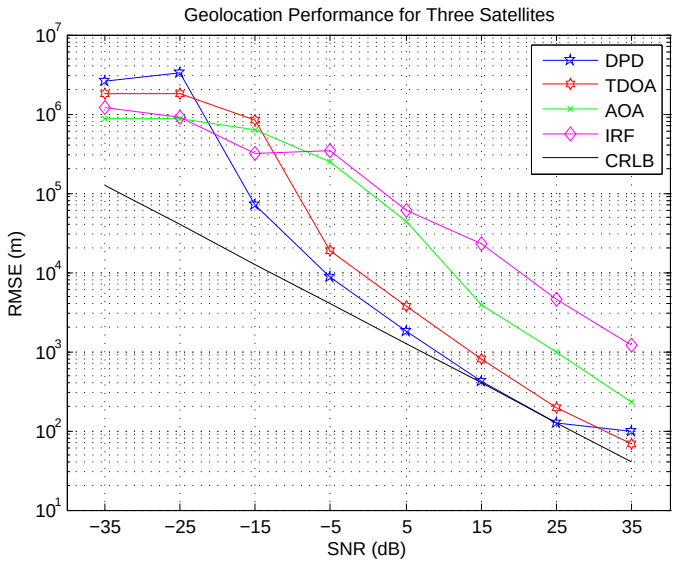


Figure 4.4: Performance of geolocation methods with a three-satellite constellation

method again outperforms the DPD method. The TDOA algorithm for three satellites includes the constraint that the transmitter be located on the Earth's surface. The DPD method does not require such a constraint, so the TDOA method ultimately has more information than the DPD algorithm, leading to better performance. The DPD method consistently outperforms the TDOA method for a large range of SNR, and does so without constraints on the altitude of the emitter. If the emitter does not lie on the surface of the earth, then the TDOA method cannot reliably be used with only three satellites.

The trade space for a three satellite system has the same considerations as for two satellites. The algorithms that can be used by expanding from two to three satellites have implications for the choice of methods to use in the system. The DPD and TDOA methods only require a single receiving antenna per sensor, with an additional cross-link antenna required if processing is completed on-board. The computational power required for the DPD method is similar to the IRF method; a grid of CAF values must be populated and exhaustively searched for each possible emitter position at each time epoch. The

computational requirements for the DPD method are typically greater than that of the TDOA, where a simple cross correlation between signals is sufficient to determine timing information. Data transfer for Weiss' DPD method would also be larger than other methods because a representation of the entire signal for each collection must be rebroadcast to a single computing element. TDOA only requires the transfer of timing information between sensors, which is a relatively small transfer. Pourhomayoun and Fowler propose methods [16] to decrease computational complexity and data transfer requirements for Weiss' DPD method. This research did not implement these proposed improvements, and further research into the implications of such modifications for a Cubesat-based geolocation mission would be appropriate. With the above considerations in mind, the DPD method has the best performance of the methods outlined, and has the potential to be an excellent method of geolocation for a space platform.

### 4.5 Scenario 4 - Four Satellites

A four satellite geolocation system allows the full use of TDOA without constraints. Additionally, it creates an over-determined solution for AOA, IRF, and DPD, which can improve the solution. The four satellites are configured in a parallelogram formation, which changes size and shape as the orbit progresses. The increase in sensors will generally decrease the PDOP for the solution, as shown in Figure 4.5.

The PDOP curve for the four-satellite constellation is similar to the three-satellite constellation, but achieves a lower minimum of 41. In order to improve the PDOP further, the distance between the satellites could be increased, improving the geometry of the constellation over the transmitter.

The performance of the algorithms is shown in Figure 4.6. The four algorithms are run in 20 trials over the range of SNR values.

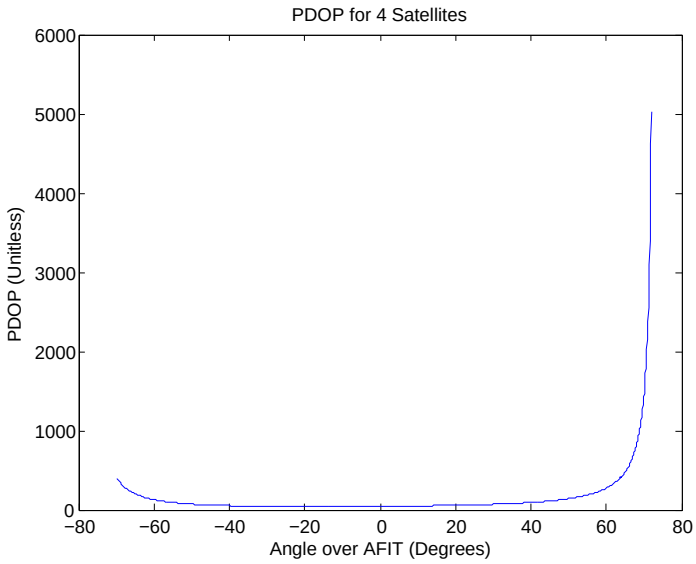


Figure 4.5: PDOP for a four satellite constellation in orbit over the target emitter

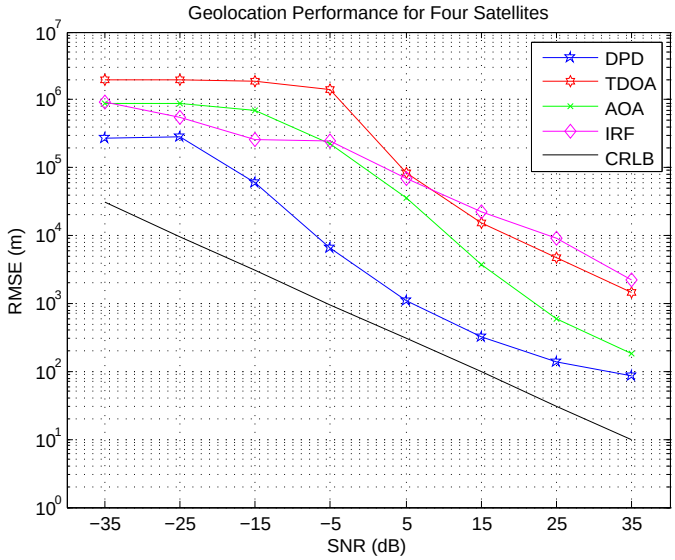


Figure 4.6: Performance of geolocation methods with a four-satellite constellation

The performance of the DPD method with four satellites in the constellation is better than the other methods by a large margin. The SNR range between -35 dB and +15 dB

again shows that the DPD method excels compared to other methods when the signal strength is low. The size of the bounding box used in the grid search methods was 200 km per side, which could model a small country. The performance of the TDOA method actually decreases in this scenario because the constraint that the emitter be on the Earth's surface is removed. Without that constraint, geolocation accuracy using the TDOA method is diminished because the range to the transmitter is so much larger than the range between satellites. If the mission designer knew the transmitter was on the surface of the Earth, the constraint could remain and the performance would likely improve slightly from the three satellite scenario.

The trade space considerations for the four satellite system are unchanged from the three satellite system. Again, DPD appears to offer the best performance, and may have the best value to a Cubesat-based geolocation system with a constellation of three or more satellites. The drawback of this method is the requirement that the signal is transmitted to a central location for processing. An example signal composed of 5000 data points in Matlab creates a file which is 30 kilobytes. A collection of 515 signal samples taken during as pass over the target would be approximately 15 megabytes in size.

## 4.6 Effects of Increasing Constellation Size for the AOA Method

The effect of adding more satellites to a geolocation system is somewhat obscured by the performance plots provided in Sections 4.2 to 4.5. In order to see the effect of adding satellites to the constellation more clearly, the results can be shown as a function of measurements per estimate rather than SNR. The SNR is held constant at +5 dB, while the number of satellites is varied from one to four. The AOA algorithm is used because it can be emlpoyed in all four scenarios. Figure 4.7 shows the convergence of the solution given for different satellite configurations.

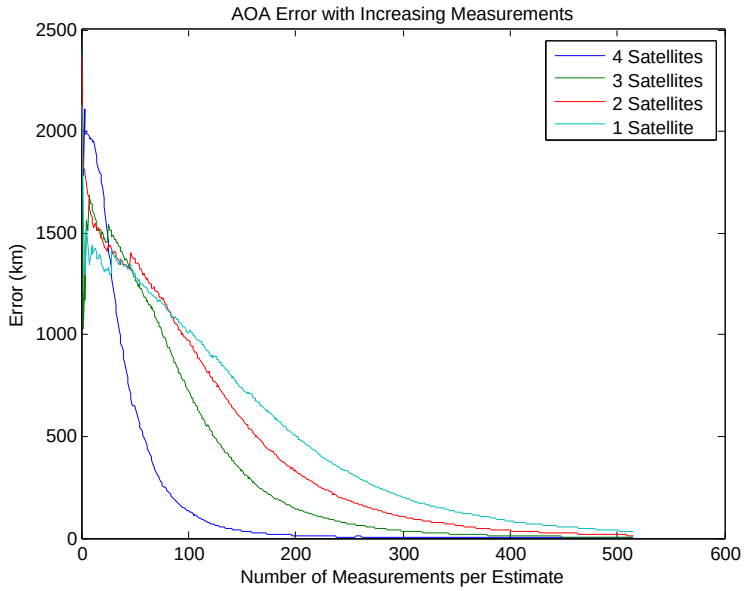


Figure 4.7: AOA Error shown as a function of the number of satellites in the system

The error shown in Figure 4.7 approaches zero as more measurements are obtained. Increasing the number of satellites decreases the time required for convergence, and results in a smaller error magnitude when convergence is achieved. When a single satellite is present, the solution doesn't really converge until the orbit is nearly complete at 515 samples. When four satellites are present, the solution converges before the orbit is halfway complete, at around 200 measurements. This is because there is four times as much information per measurement when four satellites are present, compared to a single satellite.

## 4.7 Effects of Changing the Bounding Box on DPD

The DPD and IRF methods use a grid search to perform the position calculation, using a predetermined 'bounding box' within which the emitter is assumed to be located. The bounding box is used to define initial grid parameters, and the box becomes smaller as the algorithm progresses, until the final bounding box is a cube with 10 meter sides. The initial bounding box size can be altered in the simulation to show its effect on the

performance of the locator. Figure 4.8 shows the performance of the DPD method using bounding box sizes varying from 100 m to 1000 km. Three satellites are used in each trial, with 10 trials per SNR step. The same SNR step of 10 dB is used for SNR values ranging from -35 dB to +35 dB. The grids are designed as described in Section 3.5.4, with 125 points in the grid, and decreasing in size by 20 percent per dimension in each iteration. The results are shown in Figure 4.8.

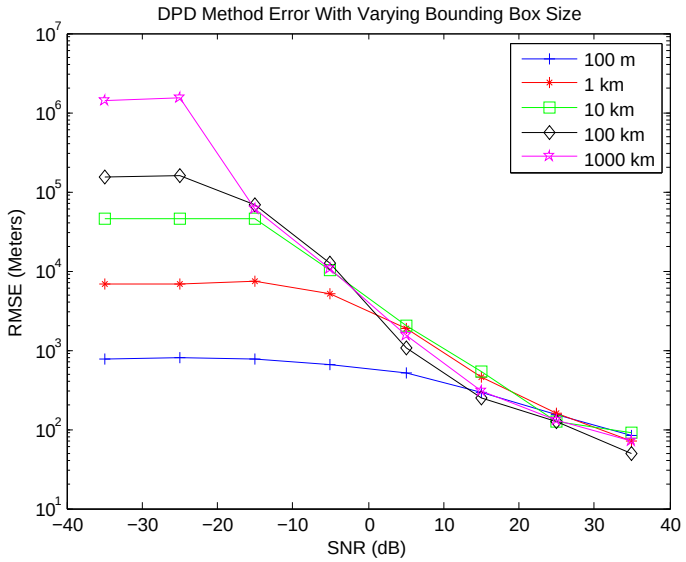


Figure 4.8: The performance of the DPD method is dependent on the size of the bounding box, especially at lower SNR values

Figure 4.8 shows that the performance of the DPD method is dependent on the bounding box used in the algorithm, as well as signal strength. The results show that the algorithm provides a solution at the edges of the bounding box when the SNR is at or below -25 dB. As the SNR improves, the solution will improve as well. The figure shows that bounding boxes with sides smaller than 10 km have a bias even when SNR is greater than -15 dB. The bounding box must be taken into consideration when designing a geolocation mission using the DPD or IRF method because the algorithm relies so heavily

on the correct placement and size of the search grid. If the bounding box is too small and is misplaced, the method may converge to an incorrect solution simply because the true emitter position is not present within the perimeter of the search grid. Additionally, the mission designer must assess whether Cubesat geolocation provides information if the bounding box is small. If the target position is known to be within a 1 km block, the DPD method will not provide better information than this unless the signal SNR at the receiver is greater than +15 dB.

## 4.8 CRLB Analysis

The CRLB for each parameter is calculated. The CRLB for bearing measurements offers interesting results for the case of a fixed orbit. A normal orbit has a period of time where the satellite is approaching the target and a period of time when the satellite is moving away from the target. The lower bound of the bearing estimation accuracy is highly dependent on the true angle from which the signal is arriving. The bearing estimation accuracy is maximized when the signal arrives at the antenna array when the satellite reaches zenith relative to the target emitter. The bearing estimate accuracy reaches a minimum when the signal reaches the the array at 0°. The CRLB for the elevation angle illustrated in Figure 4.9 showcases this phenomenon for an SNR of +15 dB. When the signal is initially received by the sensor as it orbits, the target is presumably on or near the horizon. When the satellite reaches the smallest distance from the target, the estimate will be much more reliable because the true elevation angle will be higher. Figure 3.3 showed that the satellites in this research will not pass directly overhead the target, so the elevation angle will not reach 90°. However, Figure 4.9 shows that as the satellite approaches the target, the CRLB will decrease, and as the satellite moves away from the target, the CRLB will increase again.

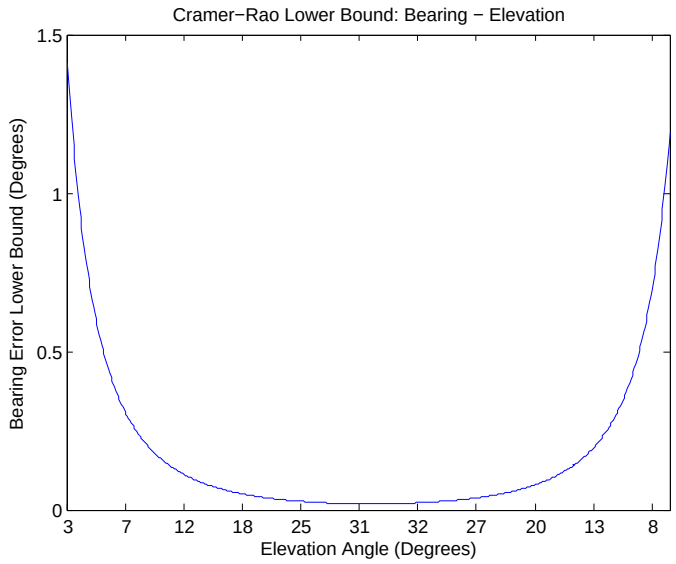


Figure 4.9: The elevation angle CRLB calculated over one pass will decrease as the true bearing angle increases toward 90°, then increase again as the bearing angle decreases toward 0°

This research assumes that one set of sensing antennas is placed facing nadir, and one set is placed 90° offset from nadir. Additionally, the satellite is assumed to have enough fuel to perform station-keeping maneuvers throughout its lifetime. The azimuth bearing for this particular scenario never reaches 0°, and fares much better than the elevation angle throughout the orbit, as shown in Figure 4.10. The orientation of the antennas on the satellite's frame will have an effect on the angle at which the signal is sensed as well, and could change this CRLB significantly.

The frequency and timing lower bounds do not change with target-to-satellite geometry as with the lower bound on bearing angles. As detailed in Section 3.6.1.1, the lower bounds for frequency and timing are dependent on signal parameters such as SNR and bandwidth. Figure 4.11 and Figure 4.12 show the CRLB on standard deviation calculated for the frequency measurement and timing measurement, respectively.

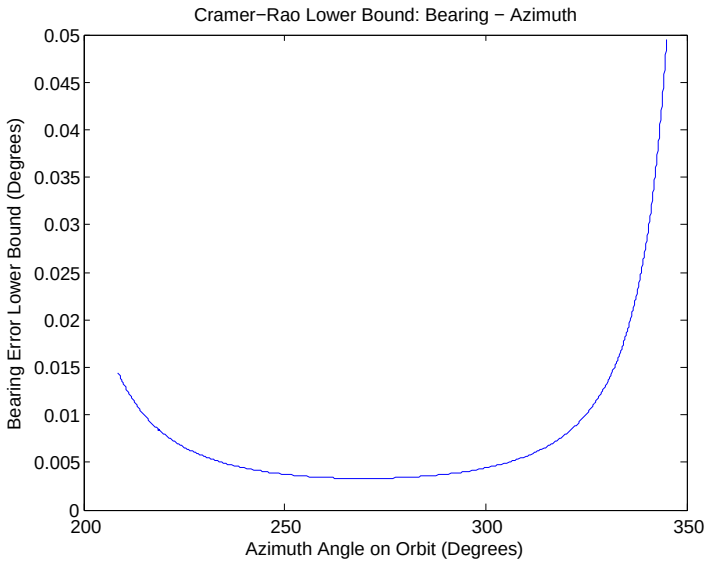


Figure 4.10: CRLB calculated for azimuth angle estimation over one orbit

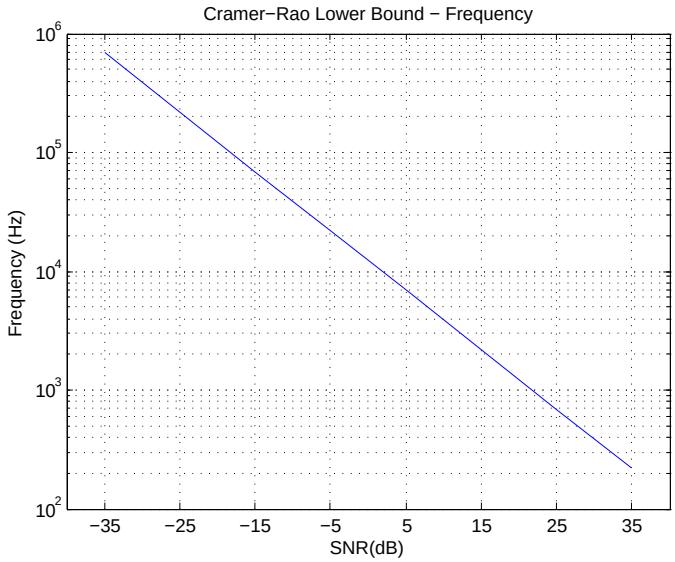


Figure 4.11: CRLB calculated for frequency measurement at a range of SNR values

Figure 4.11 shows that the frequency measurement for this simulation has a statistical lower bound of about 200 Hz at an SNR of +35 dB. The timing measurement has a

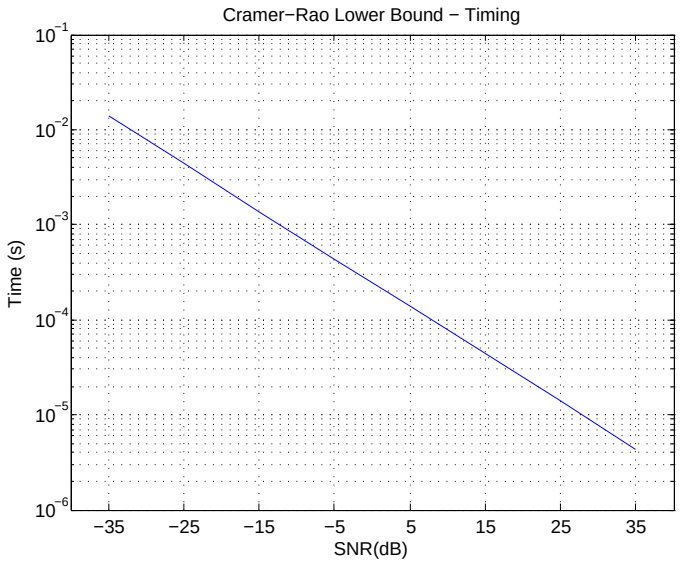


Figure 4.12: CRLB calculated for timing measurement at a range of SNR values

statistical lower bound of about 40 microseconds at an SNR of +35 dB, as in Figure 4.12. These figures could be improved by increasing the bandwidth of the signal and the duration of the collection.

## 4.9 PDOP Results

The PDOP calculated for the satellite constellation configurations used in this research shows the effect geometry has on the performance of the algorithms. As the results in the previous section showed, adding more satellites will promote a faster convergence to a geolocation solution. Figure 4.13 shows the PDOP calculated for the scenarios with three and four satellite constellations (PDOP cannot be reasonably computed for fewer than three satellites).

The PDOP is shown to be a curve, where the orbit has the lowest PDOP at zenith. The best geometry is at the center of the orbit because the ratio between the target range

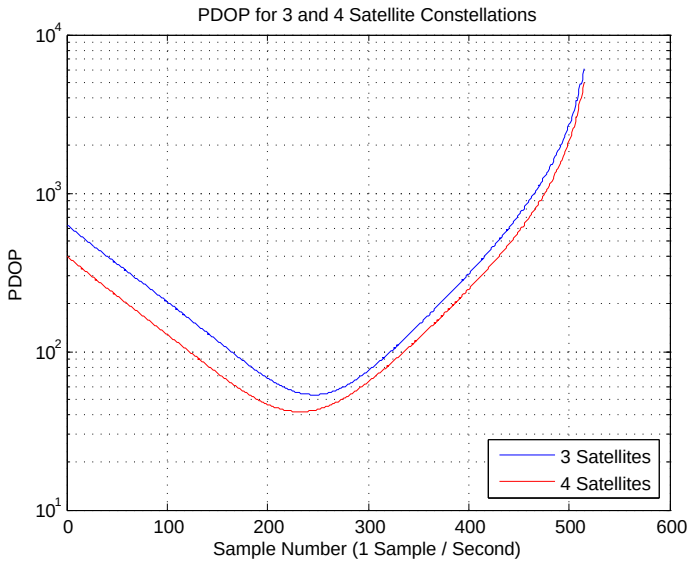


Figure 4.13: Adding satellites to the geolocation constellation is shown to improve PDOP

and the satellite separation is at its smallest. According to Langley, DOP will always decrease when more sensors are present [42].

By way of comparison, the PDOP is poor for all of the scenarios discussed in this chapter compared to the PDOP that a typical GPS receiver has. GPS typically has DOP measurements less than 10, whereas this system has a minimum PDOP of 41. There are elements of the design that favor smaller distances between satellites, which will increase the PDOP. For example, communication links between satellites are more effective at smaller distances, and could constrain the geometry. A smaller constellation geometry may also increase the time in which all the satellites receive the SOI. The orbital dynamics of the geolocation system must be carefully planned to balance the needs of the satellite constellation with the desire to minimize the dilution of precision and thereby improve the position estimate.

## 4.10 Summary

The results and analysis presented in this chapter characterizes the performance of four geolocation algorithms applied to a number of sensors orbiting over an RF emitter. The analysis of the scenarios shows that the DPD method generally performs better than the IRF method, as well as the classical methods of TDOA and AOA. The performance gained by using DPD at lower SNR values, especially in the region from -15 to +15 dB, is significant. A geolocation mission using Cubesats would gain a substantial improvement in performance by implementing the DPD algorithm.

Several considerations for the selection of a geolocation method are addressed in this research. The hardware requirements for the AOA method include an antenna array rather than a single antenna, which is a burden for such a small satellite architecture. When multiple satellites are present, a cross-link radio and antenna are required to share information between the satellites. The DPD method presented by Weiss is more computationally complex and requires more data transfer than the other methods considered, but these issues may be diminished by implementing the approximated DPD method proposed by Pourhomayoun and Fowler [16]. This research did not use the approximated DPD method, and further investigation into its performance from an orbiting sensor platform should be conducted. Given the results presented in Sections 4.2 to 4.5, the IRF method is suggested for consideration for single satellite and two satellite constellations. The DPD method is recommended for use, versus TDOA, for constellations with three or more satellites.

The results presented in this thesis are comparable with other results in open literature [18], [16]. The algorithms considered in this research are shown generally to approach the CRLB, the statistical lower bound on the performance of an estimator. Other research has shown this tendency, but this research is specific to the consideration of sensors in orbit. Standoff distances on the order of one thousand kilometers have not been

previously demonstrated to work for the DPD method. This thesis is believed to present the first such results.

Chapter V provides conclusions drawn from this research and recommendations for future research.

# V. Conclusion

## 5.1 Conclusions

This research presents a simulation environment and methodology to characterize the geolocation performance of a constellation of nano-satellites in LEO. The simulation incorporated realistic orbits created in AGI's STK software to use in conjunction with four geolocation algorithms. The results of the simulation and the analysis presented in this research provide a thorough comparison of the performance that should be expected from the algorithms and methods used in a variety of scenarios. Other considerations, such as statistical lower bounds, the effect of geometry, and the number of satellites in a geolocation system are addressed with respect to the geolocation methods investigated in this research.

The evidence supports further research into the Direct Position Determination method, as it appears to perform better than other methods at the standoff range of a satellite system with three or more platforms. When a Cubesat-based geolocation system has only one or two satellites, the IRF method provides a balance between performance and hardware requirements that make it attractive for use with the nano-satellite architecture in some geolocation scenarios.

A Cubesat based geolocation system can be a powerful tool to locate terrestrial communication systems, jammers, radars, and other RF emitters. This research has displayed the use of four geolocation methods which can be used in different circumstances to locate an emitter.

When a single Cubesat is used to geolocate, the AOA and IRF algorithms may be used because the satellite has velocity while moving along its orbit. The AOA and IRF methods' performance suggest that the AOA method will generally perform better on orbit. While the AOA method outperforms the IRF method, the smaller footprint of the

hardware requirements for the IRF method make it appealing if some performance degradation is acceptable. By adding a second satellite, the performance of the AOA and IRF methods will improve, decreasing the time required to approach the CRLB. The evidence supports further research into the Direct Position Determination method, as it appears to perform better than other methods at the standoff range of a satellite system with three or more platforms. The DPD method has been shown to be effective in geolocating RF emitters at satellite-range standoff distances. When a Cubesat-based geolocation system has only one or two satellites, the IRF method provides a balance between performance and hardware requirements that make it attractive for use with the nano-satellite architecture.

## 5.2 Recommendations for Future Work

There are a number of areas in which this research should be continued and enhanced. Including a robust model for the attenuation associated with signal broadcast through the atmosphere would make the propagation of the transmitted signal more realistic. The atmospheric attenuation a signal experiences is dependent on the frequency of that signal, so an in-depth analysis of the impact on geolocation performance associated with variation in the SOI carrier frequency should be completed with use of this more robust model.

A study of the orbital properties of the system, and how they would affect the performance of geolocation would be appropriate as well. PDOP would be an important consideration in such an analysis. Additionally, more passes could be added to the simulation to show how more collected data will improve the solution.

Further improvements can be made to the algorithms used in the geolocation system. The IRF method would benefit from improving the precision and processing time for measuring the instantaneous received frequency. The approximated DPD method [16]

should be explored in detail and compared to the performance of Weiss' DPD method [18] to ensure performance degradation at standoff distances is sufficiently small.

The type of signal could be analyzed with respect to geolocation performance. This research focused on a narrowband signal with a relatively generic pulse for the signal's structure. Wideband and ultra-wideband signal sources are common in the communications field, and could present unique challenges for geolocation systems. Additionally, different modulation techniques such as Gaussian minimum shift keying (GMSK) or binary phase shift keying (BPSK) may be important factors in the design of a geolocation system.

## Bibliography


[1] U. Nagendran, "Methods of using wireless geolocation to customize content and delivery of information to wireless communication devices," 4 May 2004, US Patent 6,731,940.

[2] G. M. Djuknic and R. E. Richton, "Geolocation and assisted GPS," *Computer*, vol. 34, no. 2, pp. 123–125, 2001.

[3] I. Progri, *Geolocation of RF Signals: Principles and Simulations*. Springer, 2011.

[4] C. Gentile *et al.*, *Geolocation Techniques: Principles and Applications*. Springer, 2013.

[5] D. J. Torrieri, "Statistical theory of passive location systems," *IEEE Transactions on Aerospace and Electronic Systems*, no. 2, pp. 183–198, 1984.

[6] M. L. Fowler and X. Hu, "Signal models for TDOA/FDOA estimation," *IEEE Transactions on Aerospace and Electronic Systems*, vol. 44, no. 4, pp. 1543–1550, 2008.

[7] A. D. Stewart, "Comparing time-based and hybrid time-based/frequency based multi-platform geolocation systems," Master's thesis, Naval Postgraduate School, Monterrey, CA, 1997.

[8] K. Ho and Y. Chan, "Solution and performance analysis of geolocation by TDOA," *IEEE Transactions on Aerospace and Electronic Systems*, vol. 29, no. 4, pp. 1311–1322, 1993.

[9] R. G. Wiley, *Electronic Intelligence: The Interception of Radar Signals, vol. 1*. Dedham, MA: Artech House, Inc., 1985.

[10] C. Estrella. (2014, 28 January) Chapter 6: Emitter location. [Online]. Available: http://www.globalspec.com/reference/60402/203279/chapter-6-emitter-location

[11] C. O. Savage and B. F. La Scala, "Accurate target geolocation using cooperative observers," in *Information, Decision and Control*. IEEE, 2007, pp. 248–253.

[12] C. O. Savage, R. L. Cramer, and H. A. Schmitt, "TDOA geolocation with the unscented Kalman filter," in *Proceedings of the 2006 IEEE International Conference on Networking, Sensing and Control*. IEEE, 2006, pp. 602–606.

[13] A. Mikhalev and R. F. Ormondroyd, "Comparison of Hough transform and particle filter methods of emitter geolocation using fusion of TDOA data," in *4th Workshop on Positioning, Navigation and Communication*. IEEE, 2007, pp. 121–127.

[14] ——, "Passive emitter geolocation using agent-based data fusion of AOA, TDOA and FDOA measurements," in *10th International Conference on Information Fusion*. IEEE, 2007, pp. 1–6.

[15] O. Bar-Shalom and A. J. Weiss, "Direct position determination of OFDM signals," in *IEEE 8th Workshop on Signal Processing Advances in Wireless Communications*. IEEE, 2007, pp. 1–5.

[16] M. Pourhomayoun and M. L. Fowler, "Sensor network distributed computation for direct position determination," in *2012 IEEE 7th Sensor Array and Multichannel Signal Processing Workshop (SAM)*. IEEE, 2012, pp. 125–128.

[17] M. Oispuu and U. Nickel, "Direct detection and position determination of multiple sources with intermittent emission," *Signal Processing*, vol. 90, no. 12, pp. 3056–3064, 2010.

[18] A. J. Weiss, "Direct position determination of narrowband radio frequency transmitters," *IEEE Signal Processing Letters*, vol. 11, no. 5, pp. 513–516, 2004.

[19] D. Nelson and J. McMahon, "Target location from the estimated instantaneous received frequency," in *SPIE Defense, Security, and Sensing*, vol. 8020. International Society for Optics and Photonics, 2011, pp. 80 200Q1–80 200Q8.

[20] M. Azaria and D. Hertz, "Time delay estimation by generalized cross correlation methods," *IEEE Transactions on Acoustics, Speech and Signal Processing*, vol. 32, no. 2, pp. 280–285, 1984.

[21] S. Stein, "Differential delay/doppler ML estimation with unknown signals," *IEEE Transactions on Signal Processing*, vol. 41, no. 8, pp. 2717–2719, 1993.

[22] H. H. Jenkins, *Small-Aperture Radio Direction-Finding*. Norwood, MA: Artech House, Inc., 1991.

[23] K. T. Wong and M. D. Zoltowski, "Self-initiating MUSIC-based direction finding in underwater acoustic particle velocity-field beamspace," *IEEE Journal of Oceanic Engineering*, vol. 25, no. 2, pp. 262–273, 2000.

[24] A. Barabell, "Improving the resolution performance of eigenstructure-based direction-finding algorithms," in *IEEE International Conference on Acoustics, Speech, and Signal Processing*, vol. 8. IEEE, 1983, pp. 336–339.

[25] J. Pierre and M. Kaveh, "Experimental performance of calibration and direction-finding algorithms," in *1991 International Conference on Acoustics, Speech, and Signal Processing*. IEEE, 1991, pp. 1365–1368.

[26] R. Schmidt, "Multiple emitter location and signal parameter estimation," *IEEE Transactions on Antennas and Propagation*, vol. 34, no. 3, pp. 276–280, 1986.

[27] G. Casella and R. L. Berger, *Statistical Inference, Second Edition*. Duxbury Press, 2001.

[28] (2014, 12 February) Point closest to a set four of lines in 3D. [Online]. Available: http://math.stackexchange.com/questions/36398/point-closest-to-a-set-four-of-lines-in-3d

[29] S. Kulumani, "Space-based TDOA geolocation," 20 August 2013, AFRL/RVSV.

[30] G. W. Stewart, "Gershgorin theory for the generalized eigenvalue problem," *Mathematics of Computation*, vol. 29, no. 130, pp. 600–606, 1975.

[31] S. Stein, "Algorithms for ambiguity function processing," *IEEE Transactions on Acoustics, Speech and Signal Processing*, vol. 29, no. 3, pp. 588–599, 1981.

[32] D. Selva and D. Krejci, "A survey and assessment of the capabilities of Cubesats for Earth observation," *Acta Astronautica*, vol. 74, pp. 50–68, 2012.

[33] K. Ho *et al.*, "Source localization using TDOA and FDOA measurements in the presence of receiver location errors: Analysis and solution," *IEEE Transactions on Signal Processing*, vol. 55, no. 2, pp. 684–696, 2007.

[34] D. W. Allan, "Time and frequency (time-domain) characterization, estimation, and prediction of precision clocks and oscillators," *IEEE Transactions on Ultrasonics, Ferroelectrics and Frequency Control*, vol. 34, no. 6, pp. 647–654, 1987.

[35] D. W. Allan *et al.*, *The Science of Timekeeping*. Hewlett-Packard, 1997.

[36] R. M. Barts and W. L. Stutzman, "Modeling and simulation of mobile satellite propagation," *IEEE Transactions on Antennas and Propagation*, vol. 40, no. 4, pp. 375–382, 1992.

[37] A. D. Panagopoulos *et al.*, "Satellite communications at Ku, Ka, and V bands: Propagation impairments and mitigation techniques," *IEEE Communications Surveys & Tutorials*, vol. 6, no. 3, pp. 2–14, 2004.

[38] F. Wang and K. Sarabandi, "A physics-based statistical model for wave propagation through foliage," *IEEE Transactions on Antennas and Propagation*, vol. 55, no. 3, pp. 958–968, 2007.

[39] J. Volakis and R. Johnson, *Antenna Engineering Handbook*. McGraw-Hill Professional, 2007.

[40] N. Patwari *et al.*, "Locating the nodes: Cooperative localization in wireless sensor networks," *IEEE Signal Processing Magazine*, vol. 22, no. 4, pp. 54–69, 2005.

[41] S. M. Kay, *Fundamentals of Statistical Signal Processing, Volume I: Estimation Theory*. Prentice Hall, 1993.

[42] R. B. Langley, "Dilution of precision," *GPS world*, vol. 10, no. 5, pp. 52–59, 1999.

[43] (2014, 28 January) Lecture 11: Satellite geometry and accuracy measures. [Online]. Available: http://nptel.ac.in/courses/Webcourse-contents/IIT-KANPUR/ModernSurveyingTech/lectureB_11/B_11_3GDOP.htm

[44] H. Heidt *et al.*, "Cubesat: A new generation of picosatellite for education and industry low-cost space experimentation," in *Proceedings of the 14th Annual AIAA/USU Conference on Small Satellites*, 2000, pp. 1–19.

[45] (2013, 13 October) Operationally Responsive Space office. [Online]. Available: http://ors.csd.disa.mil/mission/

[46] P. Gurfil, J. Herscovitz, and M. Pariente, "The SAMSON Project–cluster flight and geolocation with three autonomous nano-satellites," 2012. [Online]. Available: http://digitalcommons.usu.edu/smallsat/2012/all2012/56/

[47] C. Rose, "Method for single satellite geolocation of emitters using an ambiguous interferometer array," Oct 2008, uS Patent 7,436,359. [Online]. Available: https://www.google.com/patents/US7436359

[48] Symmetricom Quantum SA.45s CSAC data sheet. [Online]. Available: http://www.symmetricom.com/resources/download-library/documents/datasheets/quantum-sa45s-csac/

[49] Jackson Labs CSAC GPSDO frequency standard. [Online]. Available: http://www.jackson-labs.com/assets/uploads/main/CSAC_specs.pdf

[50] BCT XB1 data sheet. [Online]. Available: http://bluecanyontech.com/wp-content/uploads/2012/07/BCT-XB1-datasheet-1.2.pdf

[51] Earth radius. [Online]. Available: http://www.princeton.edu/~achaney/tmve/wiki100k/docs/Earth_radius.html

[52] P. Welch, "The use of fast Fourier transform for the estimation of power spectra: A method based on time averaging over short, modified periodograms," *IEEE Transactions on Audio and Electroacoustics*, vol. 15, no. 2, pp. 70–73, 1967.

[53] M. Fowler. (2010, 12 December) EECE 522 course notes. [Online]. Available: http://www.ws.binghamton.edu/fowler/fowler%20personal%20page/EE522.htm

[54] F. Gustafsson and F. Gunnarsson, "Mobile positioning using wireless networks: possibilities and fundamental limitations based on available wireless network measurements," *Signal Processing Magazine, IEEE*, vol. 22, no. 4, pp. 41–53, 2005.

# REPORT DOCUMENTATION PAGE

*Form Approved*
*OMB No. 0704–0188*



| 1. REPORT DATE *(DD–MM–YYYY)* | 2. REPORT TYPE | 3. DATES COVERED *(From — To)* |
|---|---|---|
| 27–03–2014 | Master's Thesis | Oct 2012–Mar 2014 |

**4. TITLE AND SUBTITLE**

Radio Frequency Emitter
Geolocation Using Cubesats

**5a. CONTRACT NUMBER**

**5b. GRANT NUMBER**

**5c. PROGRAM ELEMENT NUMBER**

**6. AUTHOR(S)**

Small, Andrew J., Captain, USAF

**5d. PROJECT NUMBER**

**5e. TASK NUMBER**

**5f. WORK UNIT NUMBER**

**7. PERFORMING ORGANIZATION NAME(S) AND ADDRESS(ES)**

Air Force Institute of Technology
Graduate School of Engineering and Management (AFIT/EN)
2950 Hobson Way
WPAFB, OH 45433-7765

**8. PERFORMING ORGANIZATION REPORT NUMBER**

AFIT-ENG-14-M-68

**9. SPONSORING / MONITORING AGENCY NAME(S) AND ADDRESS(ES)**

Air Force Research Lab
Dr. Alan Lovell, Chief, AFRL/RVSV
Thomas.lovell@kirtland.af.mil
DSN: 263-4132

**10. SPONSOR/MONITOR'S ACRONYM(S)**

AFRL/RVSV

**11. SPONSOR/MONITOR'S REPORT NUMBER(S)**

**12. DISTRIBUTION / AVAILABILITY STATEMENT**

DISTRIBUTION STATEMENT A:
APPROVED FOR PUBLIC RELEASE; DISTRIBUTION UNLIMITED

**13. SUPPLEMENTARY NOTES**



**14. ABSTRACT**

The ability to locate an RF transmitter is a topic of growing interest for civilian and military users alike. Geolocation can provide critical information for the intelligence community, search and rescue operators, and the warfighter. The technology required for geolocation has steadily improved over the past several decades, allowing better performance at longer baseline distances between transmitter and receiver. The expansion of geolocation missions from aircraft to spacecraft has necessitated research into how emerging geolocation methods perform as baseline distances are increased beyond what was previously considered. The Cubesat architecture is a relatively new satellite form which could enable small-scale, low-cost solutions to USAF geolocation needs.

This research proposes to use Cubesats as a vehicle to perform geolocation missions in the space domain. The Cubesat form factor considered is a 6-unit architecture that allows for 6000 $cm^3$ of space for hardware. There are a number of methods which have been developed for geolocation applications. This research compares four methods with various sensor configurations and signal properties. The four methods' performance are assessed by simulating and modeling the environment, signals, and geolocation algorithms using Matlab.

The simulations created and run in this research show that the angle of arrival method outperforms the instantaneous received frequency method, especially at higher SNR values. These two methods are possible for single and dual satellite architectures. When three or more satellites are available, the direct position determination method outperforms the three other considered methods.

**15. SUBJECT TERMS**

Geolocation, Cubesat, Direct Position Determination, Angle of Arrival, Time Difference of Arrival, Instantaneous Received Frequency

| 16. SECURITY CLASSIFICATION OF: | | | 17. LIMITATION OF ABSTRACT | 18. NUMBER OF PAGES | 19a. NAME OF RESPONSIBLE PERSON |
|---|---|---|---|---|---|
| a. REPORT | b. ABSTRACT | c. THIS PAGE | | | Maj Marshall Haker (ENG) |
| U | U | U | UU | 101 | 19b. TELEPHONE NUMBER *(include area code)* (937) 255-3636 x4603 marshall.haker@afit.edu |